Design of a Modular Ankle-Foot Orthosis

Undergraduate Thesis

In Partial Fulfillment of the Requirements for Graduation with Research Distinction in Mechanical Engineering at The Ohio State University

By: Alivia Lahr

The Ohio State University

2018

Thesis Committee:

Robert Siston, Advisor, Ph.D

Sandra Metzler, Ph.D

Abstract:

Ankle-foot orthotics (AFOs) are the most commonly prescribed orthotic and aid patients of all ages. There are two types of AFOs: pre-fabricated and custom. Pre-fabricated AFOs are low cost ($60), but have little success in patient treatment. Custom AFOs are expensive ($750-$1000), but required in 82% of cases due to the complexity of fit, support, and force application requirements. AFOs require replacement every 6-24 months due to the development of poor fit from general use and/or patient growth. Due to the high frequency of replacement, there have been many studies on custom AFO creation using additive manufacturing (AM) (i.e. 3D printing) to lower the cost and time of custom AFO production. However, the cost remains high due to the required 3-D printing build chamber size, AM materials with the required material properties, and scanning software used to determine the AFO contours. The purpose of this study was to design a low cost, modular AFO that can be easily customized in size, support, and force application using a set of mass-produced components. Previously collected data was used to create a novel process for the development of interchangeable AFO components. SolidWorks and ANSYS force analysis software were used to design a modular AFO that consisted of 14 modular components. The components were further divided by size and support needs to generate a set of 62 modular components that could be used to build AFOs for pediatric patients of ages 3-11 years. The results of this study can be used in the future for the design of highly customizable, inexpensive, modular assistive devices. The modular AFO design may greatly improve the quality of life and reduce the financial burden on patients requiring custom AFOs.

Acknowledgements

I would like to thank Dr. Robert Siston for allowing me to pursue research in his lab. He has taught me a great deal about both writing and presentation skills. I would also like to thank the members of the NMBL for providing advice and feedback.

Table of Contents

Abstract	**2**
Acknowledgements	**3**
Table of Contents	**4**
List of Figures:	**5**
List of Tables:	**7**
1.Introduction	**8**
1.1 Focus of Thesis	**12**
1.2 Significance of Research	**12**
1.3 Organization of Thesis	**13**
2. Methodology	**14**
2.1 Functional Requirements	**16**
2.2 Size Requirements and Failure Criteria	**25**
2.3 Evaluation of Functional Requirements	**35**
2.3.1 Functional Requirements: Size	**36**
2.3.2 Functional Requirements: Failure Criteria	**45**
2.4 FEA Validation	**58**
Chapter 3: Discussion	**61**
3.1 Modular Components	**61**
3.2 Easily Interchangeable Components	**62**
3.3 Low-Cost: Materials	**63**
3.4 Limitations	**63**
4. Conclusions	**64**
4.1 Contributions	**64**
4.2 Future Work	**65**
4.3 Summary	**65**
References:	**66**

List of Figures:

Figure 1.1: Ankle Foot Orthotic Three-Point Force Application 9

Figure 1.2: Custom Ankle Foot Orthotic Casting 10

Figure 2.1: Original Methodology Overview 14

Figure 2.2: Revised Methodology Overview 15

Figure 2.3: Equinus Deformity 17

Figure 2.4: Crouch Gait 18

Figure 2.5: Critical Joints of the Ankle-foot Complex 19

Figure 2.6: Static Foot Alignment Force Application 20

Figure 2.7: Adduction and Abduction of Foot 21

Figure 2.8: Corrective Force: Adduction (Left) and Abduction (Right) 22

Figure 2.9 Force Application for Correction of Excess Ankle Eversion (left) and Ankle Inversion (right) 23

Figure 2.10: Force Application for plantar and dorsiflexion correction 24

Figure 2.11: Ankle-foot Orthosis Trimlines 25

Figure 2.12: HUMAN SHAPES 3-year old model output 28

Figure 2.13: HUMAN SHAPES CAD model measurements 29

Figure 2.14: Location of interface pressure measurements:
A.Inner Plantar Mid-foot | B.Inner Medial Metatarsal | C.Ankle/Side of Heel 30

Figure 2.15: ANSYS Stiffness Model Boundary Conditions 32

Figure 2.16: ANSYS Stiffness Model Vertical Displacement Output 32

Figure 2.17: Plantar flexion (Blue) and Dorsiflexion Corrective Moment (Red) 33

Figure 2.18: Dorsiflexion (Blue) and Plantar flexion Corrective Moment (Red) 33

Figure 2.19: Assembly and Exploded View of Modular AFO components 35

Figure 2.20: Lateral and Medial Ankle Support Components 36

Figure 2.21: Lateral and Medial Mid-Foot Support Components 37

Figure 2.22: Lateral and Medial Metatarsal Support Components 38

Figure 2.23: Dimensions of Heel Cup and Calf Bar 39

Figure 2.24: Foot Bar and Footplate Dimensions 41

Figure 2.25: Modular AFO Calf Band 43

Figure 2.26: A. AFO structural support components

B. AFO Medial/Lateral support components 45

Figure 2.27: Constraints and Loads applied to Ankle Support Plates 47

Figure 2.28: Lateral Ankle Support Plate Von Mises Stress Contour Plot 47

Figure 2.29: Medial Ankle Support Plate Von Mises Stress Contour Plot 48

Figure 2.30: Constraints and Loads applied to Mid-foot Support Plates 49

Figure 2.31: Lateral Mid-Foot Support Plate Von Mises Stress Contour Plot 49

Figure 2.32: Medial Mid-Foot Support Plate Von Mises Stress Contour Plot 50

Figure 2.33: Constraints and Loads applied to Metatarsal Support Plates 51

Figure 2.34: Medial Metatarsal Support Plate Von Mises Stress Contour Plot 51

Figure 2.35: Lateral Metatarsal Support Plate Von Mises Stress Contour Plot 52

Figure 2.36: Boundary and Loading Conditions for AFO assembly 53

Figure 2.37: Deflection Plot of AFO Stiffness 54

Figure 2.38: Von Mises Stress Contour Plot of Externally Applied Moment 55

Figure 3.1: Modular Components to Treat Ankle Inversion/Eversion 59

List of Tables:

Table 1.1: Prefabricated vs. Custom Ankle-Foot Orthoses 9

Table 2.1: Male Pediatric Anthropometric Data Summary 26

Table 2.2: Female Pediatric Anthropometric Data Summary 27

Table 2.3: Adult Anthropometric Data Summary 27

Table 2.4: Results for 3-year old and Adult male 29

Table 2.5: Average Pressures to Foot Regions During Gait 31

Table 2.6: Overview of Ankle-Foot Orthosis Torsional Stiffness 31

Table 2.7: Pediatric Lateral/Medial Ankle Support Component Size Summary 36

Table 2.8: Pediatric Lateral/Medial Mid-foot Support Component Size Summary 37

Table 2.9: Pediatric Lateral/Medial Metatarsal Support Component Size Summary 38

Table 2.10: Pediatric Heel Cup and Calf Bar Support Component Size Summary 40

Table 2.11: Pediatric Foot Bar and Footplate Component Size Summary 42

Table 2.12: Calf Band Size 43

Table 2.13: Summary of ANSYS material model input values 45

Table 2.14: Parameters for 3-year old and Adult patients 46

Table 2.15: ANSYS Outputs for Adult AFO Component Analysis 53

Table 2.16: Modular AFO Calculated Torsional Stiffness Results 55

Table 2.17: Summary of Hand Calculation Results 56

Table 3.1: Summary of Material Cost and Manufacturing Methods 60

1.Introduction

Ankle-foot orthoses (AFOs) are external braces worn on the foot and lower leg to support the ankle joint by positioning the foot relative to lower leg. They are the most common orthotic device; accounting for approximately 26% of the 5 million orthotic devices prescribed in the United States each year [1,2]. AFOs improve the quality of life for a large and diverse patient population in terms of both age and treatment needs. Of the patient populations that utilize AFOs, 37% are pediatric (0-18 years), 36% are adult (19-65 years), and 27% are geriatric (over 65 years)[1]. AFOs are used to treat gait impairments resulting from trauma, stroke, multiple sclerosis, cerebral palsy, arthritis, posterior tibial tendon dysfunction, and flatfoot deformity [3–5]. AFOs assist the gait of patients with these disorders by controlling the ankle position through manipulation of the joint's range of motion. They also mechanically compensate for muscle weakness through a three-point force application to the ankle joint axes in the frontal, sagittal, and/or transverse planes (Figure 1.1)[6].The effectiveness of force application, and consequently the degree of gait correction, is highly dependent on the mechanical properties of the AFO, such as stiffness, yield strength, and creep resistance, as well as the quality of fit[7]. Although AFOs have shown to be effective in assisting patients with gait impairments, the stability, durability, lead-time, comfort, and cost of customization are variables that remain a challenge to their production[8].

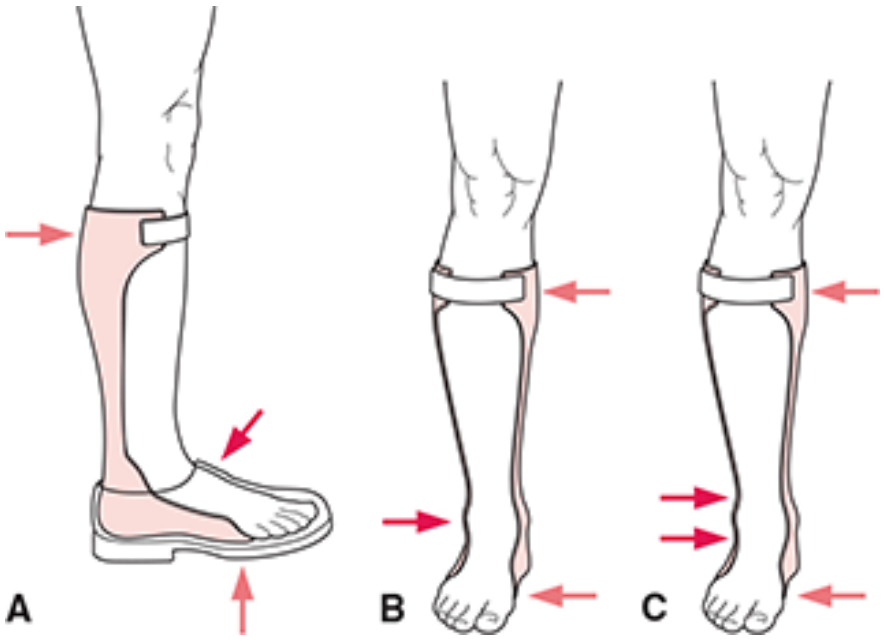

Figure 1.1: Ankle Foot Orthotic Three-Point Force Application[9]

There are two main types of AFOs: prefabricated and custom (Table 1.1). While prefabricated devices are low in cost and over-the-counter, they have a limited selection of standard sizes[7]. The standard size is selected for each patient based on shoe size, however, due to the complexity of the AFO geometry, utilizing this approach results in limited satisfaction for both patient walking ability and comfort[7,8,10]. Prefabricated AFOs are not recommended for treating complex gait issues, pediatric patients, and adult patients who weigh over 250 lbs [11]. Custom AFOs are expensive and require a time-consuming casting process to produce, but offer patient individualized fit and additional comfort[7,11]. Of the roughly 1.3 million AFOs prescribed each year, about 82% (1.066 million devices) must be customized due to the complexity of fit, support, and force application requirements[1,2].

Table 1.1: Prefabricated vs. Custom Ankle-Foot Orthoses [7,8,9]

Ankle-Foot Orthotic Type	Average Price (US $)	Fit Method	Patient Satisfaction with Comfort	Patient Satisfaction with Walking Ability
Prefabricated	60	Shoe Size	41.7%	58.3%
Custom	750-1000	Custom Casting	88.9%	100%

The production of a custom device is a complex and time-consuming process for the patient. After the patient receives a prescription for an AFO, they require an initial casting appointment (Figure 1.2) with a certified pedorthist lasting about 4 hours.

Figure 1.2: Custom Ankle Foot Orthotic Casting[12]

During this initial appointment, the pedorthist determines the contours of the foot and lower leg required for the proper force application and creates a negative mold by casting the patient's lower leg and foot. This negative mold is sent to a manufacturer where a positive mold is created, shaped and wrapped with polypropylene to form the AFO. This process has a lead-time of 1-3 weeks. Once the completed AFO is received by the

pedorthist, the patient requires a second appointment. During this second appointment, a certified pedorthist completes alterations for the final fitting of the custom AFO[3,7,11]. After completion, the patient must return to the pedorthist as needed for any additional alterations to achieve the best comfort while wearing the device.

The dynamic nature of several variables, for both the AFO and patient, may cause problems over time with fit, comfort, and force application. Due to cyclic loading from daily use and the common application of the thermoplastic polypropylene as the main material, AFOs deform over time[13,14]. When AFOs deform, their ability to provide adequate force application is compromised and they require replacement[13]. As pediatric patients grow, AFOs must be replaced so they continue to fit properly and provide the required support. AFOs typically require replacement biannually for adults and every 6-12 months for children[11]. Due to the high frequency of replacement, research has been performed to focus on lowering the cost and time associated with producing a custom AFO. The majority of these studies focused on custom AFO creation using additive manufacturing (i.e., 3D printing). The results indicate that while additive manufacturing decreases the time associated with production of AFOs (about 16.7 hours for solid polypropylene), the cost remains similar ($750-1000) to traditional manufacturing methods[3,8,15,16]. The high cost of additive manufacturing is primarily due to the required 3D printing build chamber size, the availability of additive manufacturing materials with the required material properties, and scanning software used to determine the AFO contours[3,8,17]. It was hypothesized that a combination of standard sized modular parts coupled with standard sized reinforcement components may provide the required support of a traditional thermoplastic AFO. These interchangeable parts may result in a

customizable AFO that provides similar fit and support of a traditional custom AFO, while maintaining the lower cost and shorter lead-time of prefabricated AFOs.

1.1 Focus of Thesis

The purpose of this study was to design a highly customizable, modular AFO with low-cost and easily interchangeable components. A novel process was created for the development of interchangeable components that may allow customized AFO assembly for a wide range of patient ages and sizes. Using this process, a modular AFO, and corresponding set of components, were designed and assembled in SolidWorks. The modular components were analyzed using ANSYS for both pediatric and adult patients.

1.2 Significance of Research

It has been well documented that there is a need to reduce the cost and time associated with the production of a custom AFO[3,8,18,19].The use of additive manufacturing has been thoroughly explored in relation to decreasing this time and cost, but no cost effective solution has been found[8,18]. There remains a need for a "middle-ground" design that provides higher customization, lower cost (less than $200), and a shorter lead-time (less than 8 hours).

The process of designing a modular AFO was, to the best of our knowledge, the first attempt at breaking down a custom orthotic device into interchangeable components. A modular AFO may allow pedorthists to customize each AFO design and receive immediate patient feedback in a single appointment, significantly reducing the lead-time. The utilization of mass-produced components may decrease the cost of a more customized AFO. The design of parts with ergonomic interchangeability may allow

AFOs to be easily repaired and adjusted to patient growth, changes in biomechanical requirements, or patient comfort.

1.3 Organization of Thesis

This thesis consists of 4 chapters. Chapter 2 describes the functional requirements and methodology used to design and analyze the modular components of the AFO. Chapter 3 discusses the extent of which the modular AFO design met the initial purpose of the research and associated limitations. Chapter 4, the final chapter, presents the conclusions, future work, and a summary of the thesis.

2. Methodology

The original methodology (Figure 2.1) consisted of reviewing the literature to understand how AFOs were designed to meet the requirements of each patient. Once these functional requirements were understood, a SolidWorks model of the prototype would be created and analyzed using ANSYS finite element analysis software. The prototype would then be manufactured as a proof of concept and evaluated based on the functional requirements. If the prototype passed an initial fitting and assembly test, three additional prototypes would be created for test patients to further evaluate the modular AFO functional requirements.

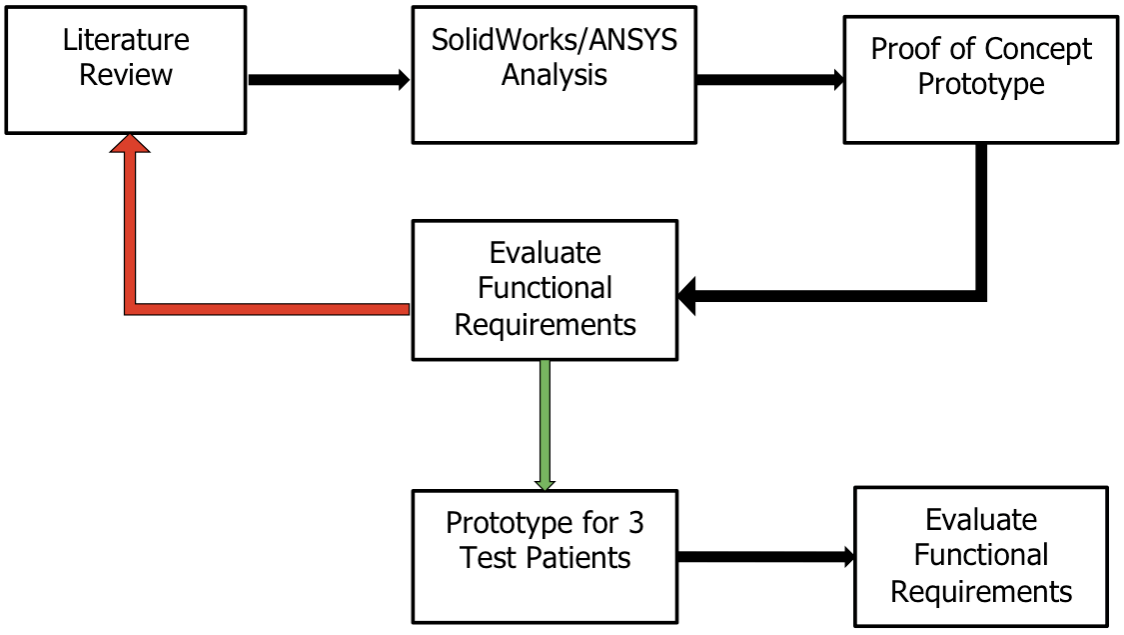

Figure 2.1: Original Methodology Overview

However, when the literature was reviewed the functional requirements and corresponding metrics were difficult to identify. The literature outlined the qualitative

processes used to manufacture standard AFOs, but lacked compiled quantitative information critical to create a design. Therefore, the methodology was revised as shown below in Figure 2.2. The revised methodology consisted of reviewing the literature and compiling quantitative information. The quantitative information was then used to outline the functional requirements and metrics that were utilized during the design process.

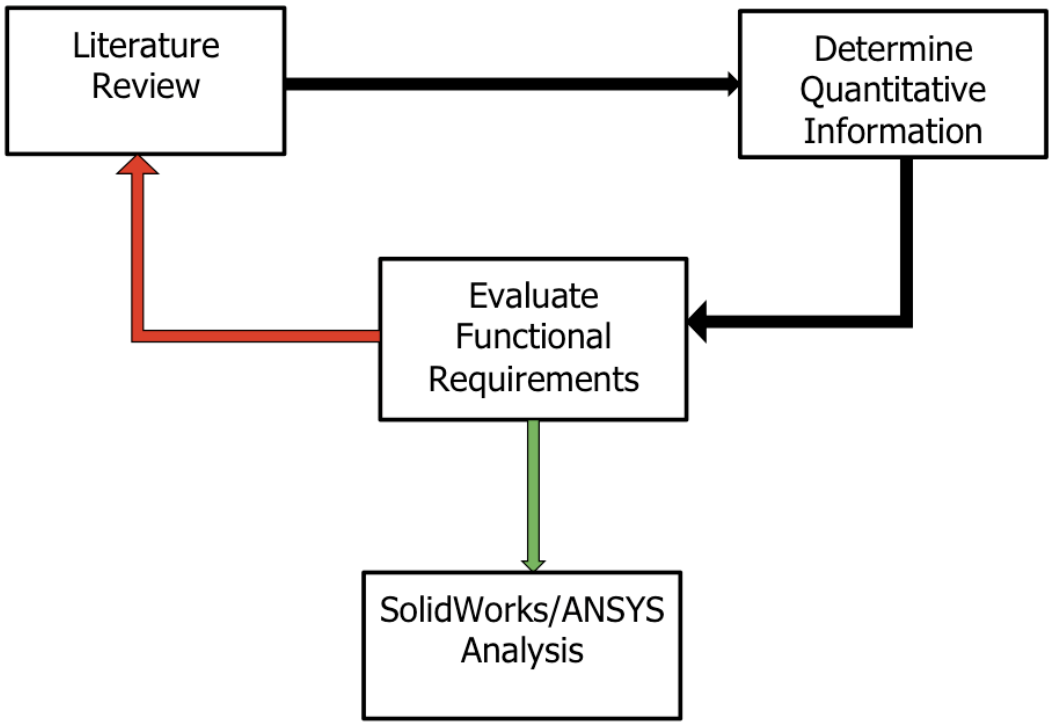

Figure 2.2: Revised Methodology Overview

2.1 Functional Requirements

Due to the wide variety of patient conditions that require custom AFOs, it was not feasible to explore the design requirements needed to treat every condition. Therefore, several simplifying assumptions were applied to narrow the functional requirement search.

The goal of the modular AFO design was to create a device that can be applied to a large portion of the patient population using the same set of components. To address the component design, the functional requirements of the patient group with the most complex needs were determined. The patient group with the most complex support requirements was ambulatory children with spastic cerebral palsy. This group was chosen as a focus for several reasons. First, the majority of AFO prescriptions are for ambulatory patients, meaning they have the ability to walk[20]. The design process behind AFOs for non-ambulatory patients is very different from that of ambulatory patients[10,21]. Second, the largest difference in size range is found amongst the pediatric population, making it the most complex sizing group[22]. Third, the most common reason for AFO prescription in pediatric patients is from gait impairment resulting from spastic cerebral palsy[2]. Based on these simplifying assumptions, the functional requirements of the modular AFO mechanics were identified.

AFOs are commonly prescribed patients with spastic cerebral palsy to treat equinus deformity and crouch gait[23,24]. Equinus is characterized by excess plantar flexion of the foot, with or without additional inversion, as shown in Figure 2.3 below. Crouch gait is characterized by excess knee flexion during the stance phase of gait resulting in excess dorsiflexion of the ankle, as shown in Figure 2.4[25].

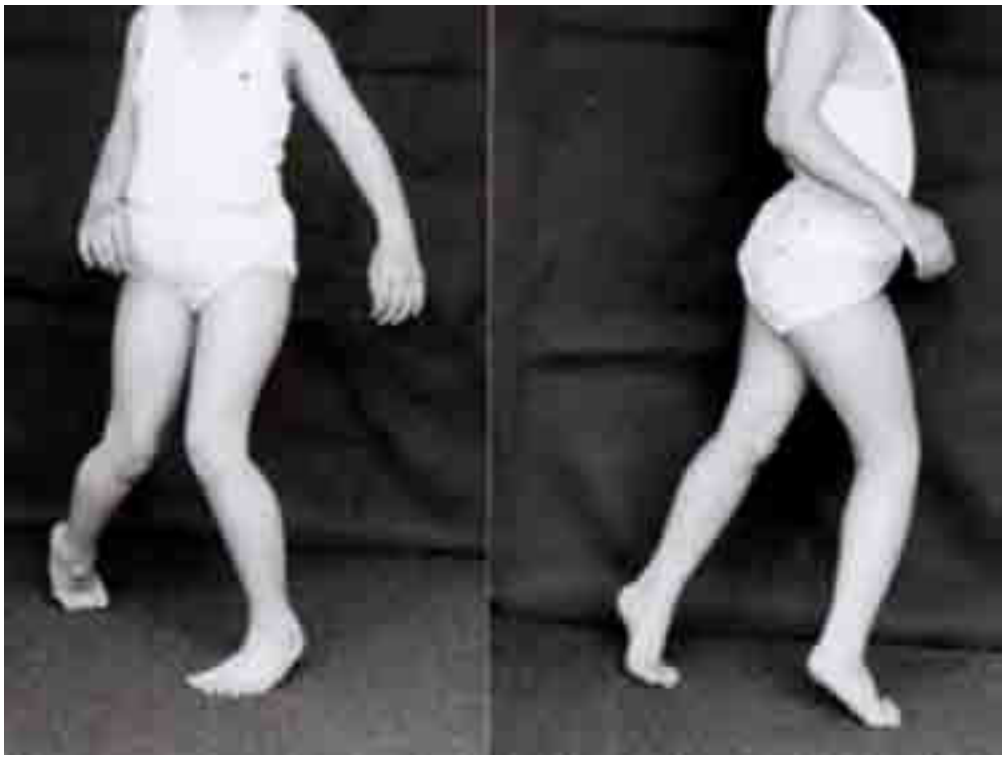

Figure 2.3: Equinus Deformity[26]

Figure 2.4: Crouch Gait[27]

AFOs control ankle position by manipulating the range of motion of the foot-ankle complex through stiffness and geometry[10]. To treat spastic cerebral palsy an AFO design must be sufficiently stiff at the ankle so that it does not buckle or flex under a plantar flexion or dorsiflexion moment[28]. This stiffness, coupled with the patient specific geometry, is required to prevent all movement of the ankle-foot complex comprised of the talo-crural, subtalar, and mid-foot joints (Figure 2.5)[28].

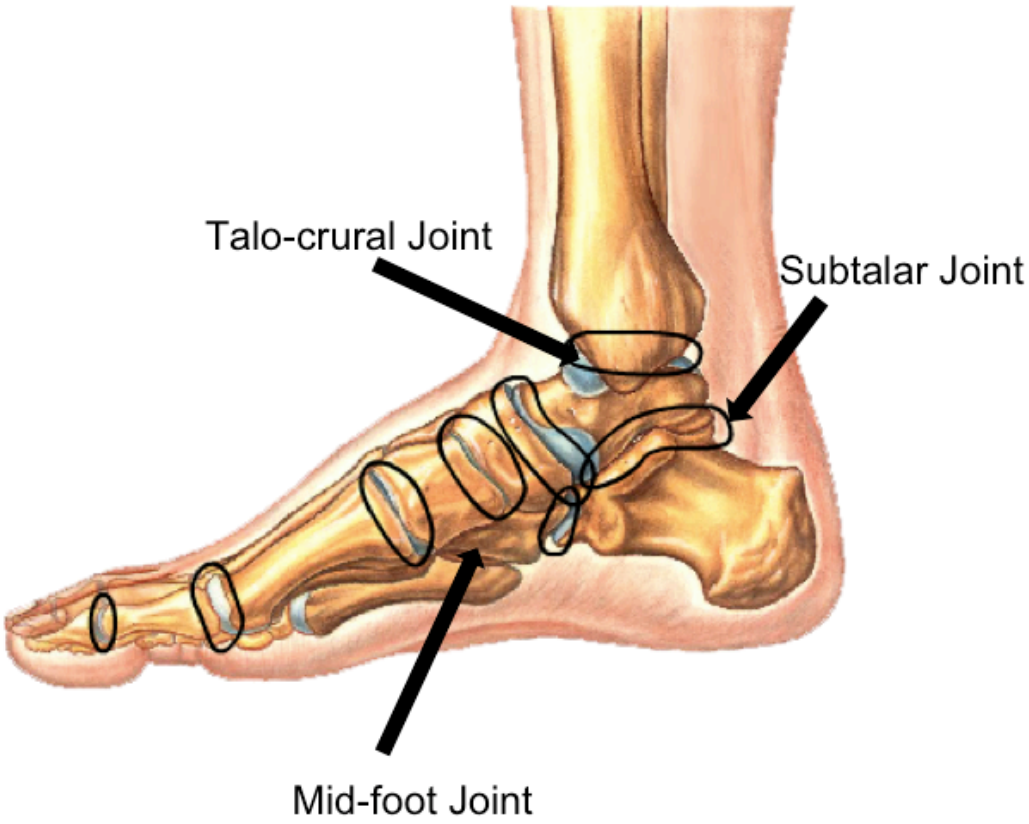

Figure 2.5: Critical Joints of the Ankle-foot Complex[29]

In the case of spastic cerebral palsy, stabilization of the ankle-foot complex requires consideration of the static foot alignment, foot abduction and adduction, ankle inversion and eversion, and ankle-foot plantar flexion and dorsiflexion[23,24,28].

Static foot alignment is defined as the neutral foot position while standing[23]. While AFOs have been shown to have no clinically significant permanent impact on static foot alignment, the correction of abnormal foot alignment is critical for the biomechanical correction of the ankle-foot complex while wearing the device[23,30]. An abnormal static foot alignment is corrected through force application to the shank of the

1st metatarsal, the head of the 5th metatarsal, and the calcaneus shown below in Figure 2.6 [31–33]. The point of force application along the 1st metatarsal is determined by the magnitude of force required to correct the deformity[31,32]. Force application to the shank of the 1st metatarsal does not create as great of a corrective moment as force application to the 1st metatarsal head due to the nature of the 3-point force application.

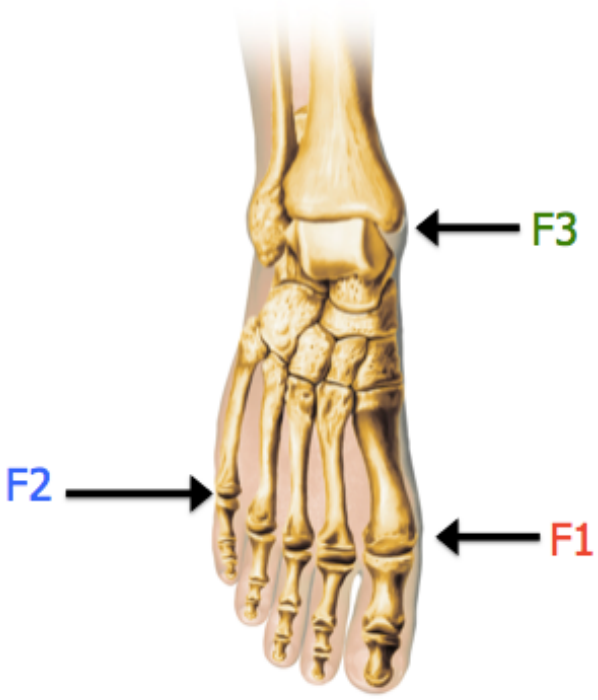

Figure 2.6: Static Foot Alignment Force Application[34]

Foot abduction is characterized by rotation of the foot along the horizontal plane away from the midline. Foot adduction is characterized by rotation of the foot along the horizontal plane toward the midline[32]. For both abduction and adduction, any excess rotation along the horizontal plane places stress on foot ligaments, resulting in instability at the ankle[35]. Representations of adduction and abduction are shown below in Figure 2.7.

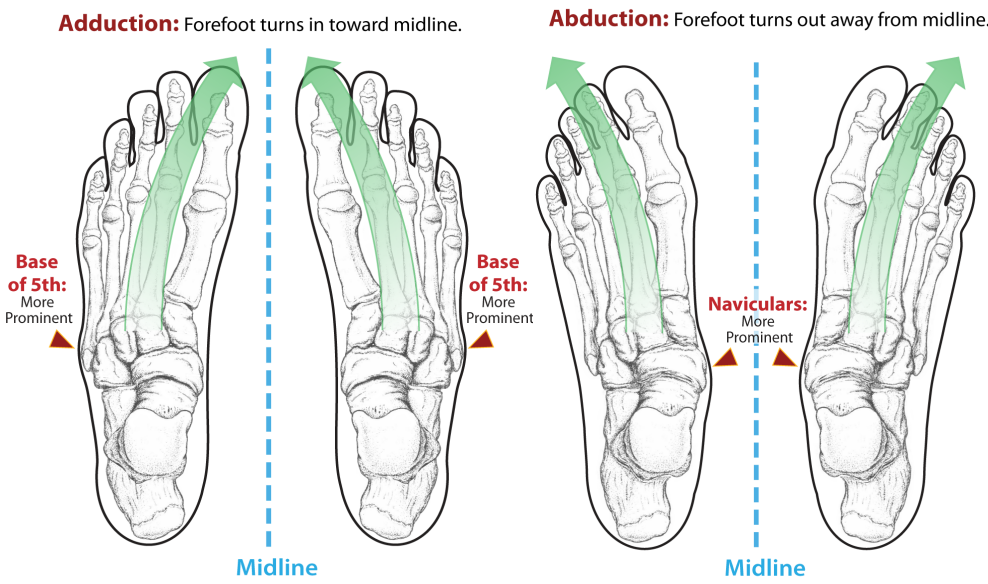

Figure 2.7: Adduction and Abduction of Foot[36,37]

Excessive foot abduction is corrected through forces applied to the 5th metatarsal head, proximal to the medial malleolus, and lateral to the lower leg. Foot adduction is corrected through forces applied to the 1st metatarsal head, proximal to the lateral malleolus, and medial to the lower leg (Figure 2.8)[31,32].

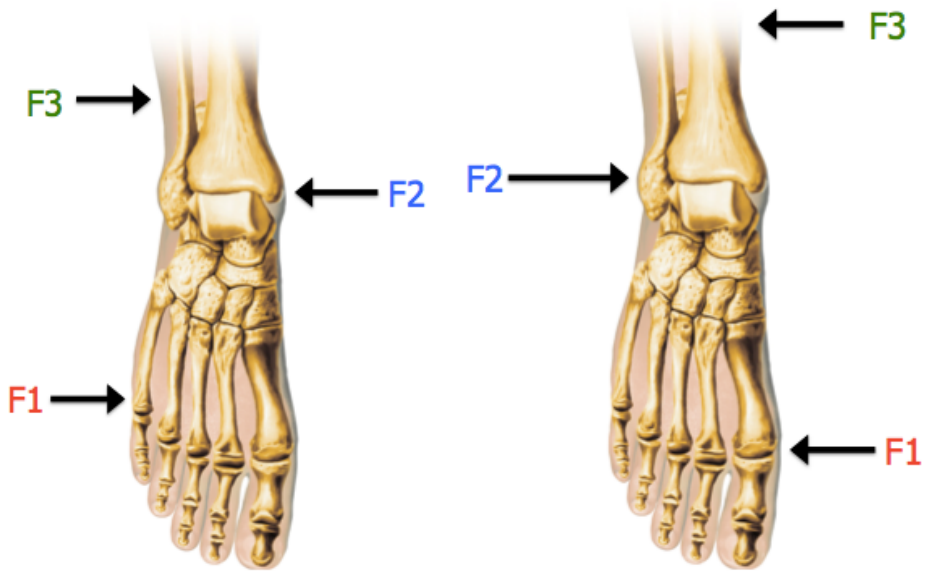

Figure 2.8: Corrective Force: Adduction (Left) and Abduction (Right)[34]

Ankle inversion is characterized by rotation of the soles of the foot inward, while ankle eversion is characterized by rotation of the soles of the foot outward[32]. Chronic excess inversion or eversion results in ankle instability and increased strain on different ligaments in the foot[31,32]. Excess ankle eversion is corrected through three point force application to the head of the 5th metatarsal, the soft tissue 1 cm anterior to the medial malleolus, and the proximal lateral calf, shown below in Figure 2.9. Excess ankle inversion is corrected through three point force application to the shaft of the 1st metatarsal, the soft tissue at least 1 cm anterior to the lateral malleolus, and the proximal medial calf, shown below in Figure 2.5[31,32,38,39].

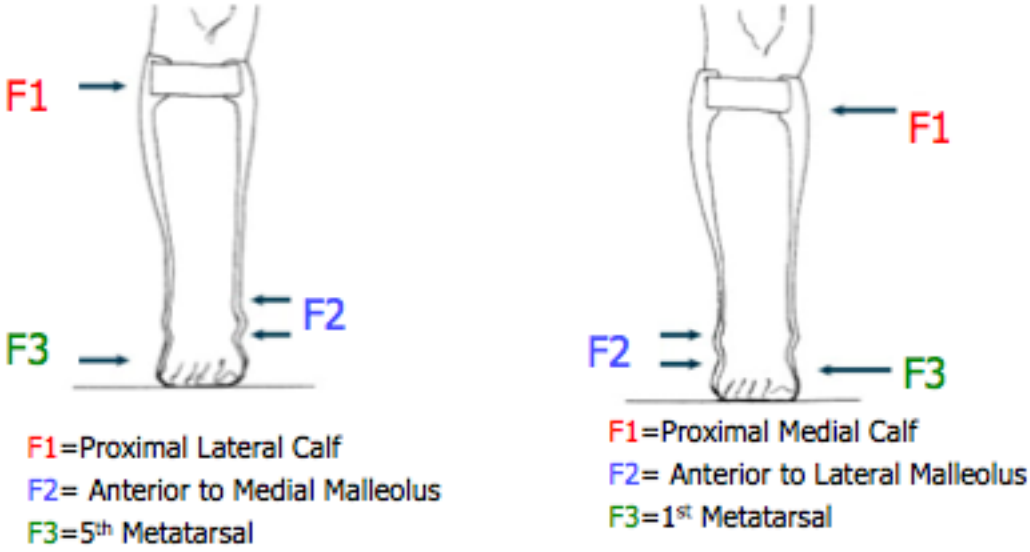

Figure 2.9 Force Application for Correction of Excess Ankle Eversion (left) and Ankle Inversion (right)[32]

The dorsiflexion and plantar flexion correction is critical to ambulatory patients[20]. The stabilization of the ankle-foot complex allows the degree of dorsi/plantar flexion to be corrected. Three-point force application is used to limit excess dorsi/plantar flexion through force application along the metatarsal line, 90 degrees to mid-foot, and on the posterior calf at least 1 cm below the fibular head (Figure 2.10)[28,32,39,40]. The location of the force application is dependent upon the corrective moment required and the pressure limits of soft-tissue[41,42].

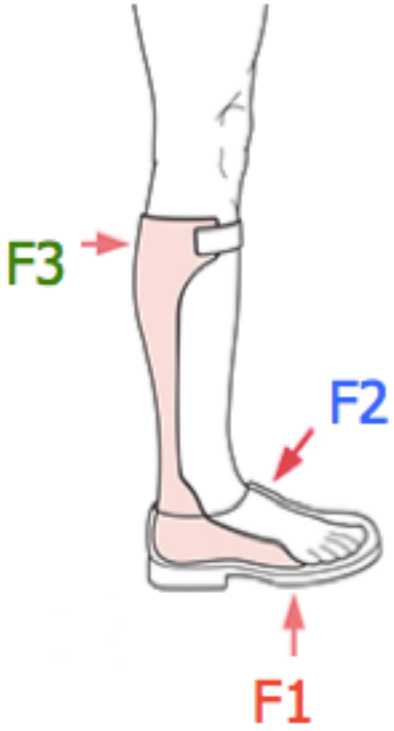

Figure 2.10: Force Application for plantar and dorsiflexion correction[32]

For traditional thermoplastic AFOs, the magnitude and location of force application is dictated by the geometry of the AFO perimeter, called the trimline[43,44]. The overall trimline of an AFO consists of five parts: proximal trimline, anterior trimline, ankle trimline, foot trimline, and metatarsal trimline, shown below in Figure 2.11[32,43]. Because AFOs provide support by three-point force application, the trimline geometry has a large impact on the resulting AFO stiffness, as well as the pressure placed on patient tissue[43,45].

Figure 2.11: Ankle-foot Orthosis Trimlines[32]

2.2 Size Requirements and Failure Criteria

To determine the size and geometry of the modular components the critical anthropometric dimensions of the AFO components were identified by the location of force application and traditional AFO mechanics, as discussed in section 2.1.

The size requirements were determined from the 50th percentile of the anthropomorphic data from the CDC Anthropometric Reference Data for Children and Adults[22]. The University of Michigan's software HUMAN SHAPES was used to convert the anthropometric data to body segment lengths for children ages 3-11 and average adult males and females from ages 20-80 years. The software required input variables of

subject height, body mass index, and ratio of sitting height to standing height[46–49]. A summary of the software input variables is shown Tables 2.1 -2.3.

Table 2.1: Male Pediatric Anthropometric Data Summary[22,49]

Age	Standing Height (in)	Sitting/Standing Height	Body Mass Index
3	38.9	0.572	16.0
4	41.7	0.555	15.8
5	44.5	0.546	16.1
6	47.0	0.541	16.0
7	49.1	0.536	16.2
8	51.7	0.531	16.6
9	53.8	0.525	17.1
10	56.1	0.520	17.9
11	58.8	0.516	20.5

Table 2.2: Female Pediatric Anthropometric Data Summary[22,49]

Age	Standing Height (in)	Sitting/Standing Height	Body Mass Index
3	39.0	0.568	15.9
4	41.2	0.553	15.9
5	44.1	0.546	15.6
6	46.8	0.541	15.9
7	49.3	0.536	16.1
8	51.5	0.531	17.1
9	53.8	0.526	18.3
10	56.9	0.522	19.1
11	59.3	0.519	19.3

Table 2.3: Adults 20-80 Anthropometric Data Summary[22]

Sex	Standing Height (in)	Sitting/Standing Height	Body Mass Index
Female	63.7	0.520	27.7
Male	69.1	0.520	27.7

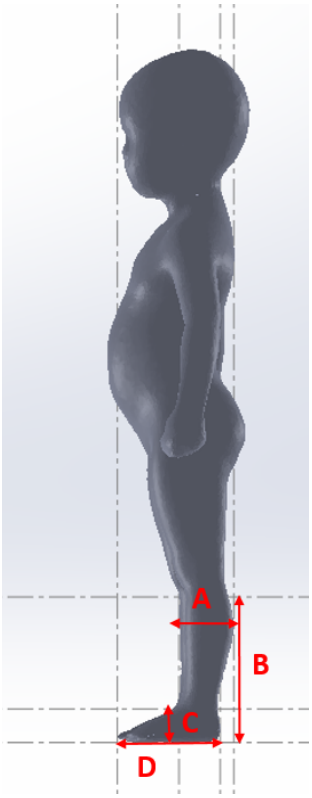

Figure 2.12: HUMAN SHAPES 3-year old model output

HUMAN SHAPES generated a statistical computer-aided design (CAD) model based on the input parameters, as well as a list of coordinates for significant landmarks. The CAD model was used to determine the calf diameter (A), shaft length (B), navicular height (C), and foot length (D) (Figure 2.12). The landmark coordinates were used to determine the height of the medial and lateral malleoli.

To complete failure analysis on the modular components, the bounds of the patient height range were identified. The lower bound was the 3-year old male group and the upper bound was the 20-80 year old male group. Figure 2.13 shows the location of the measurements taken from the CAD model and Table 2.4 summarizes the results for the 3-year old male and adult (20-80 year) male information.

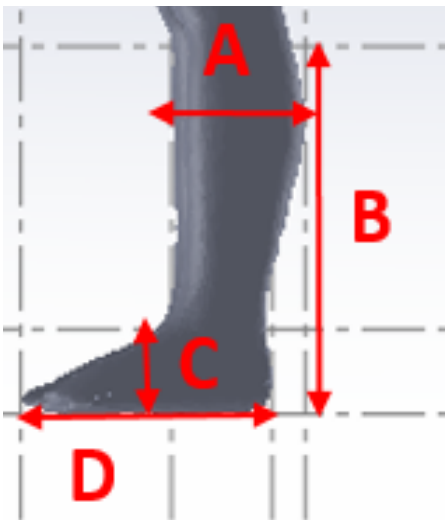

Figure 2.13: HUMAN SHAPES CAD model measurements

Table 2.4: Results for 3-year old male and Adult male

	A	B	C	D	Landmark Data	
Patient Age (Years)	Calf Diameter (in)	Shaft Length (in)	Navicular Height (in)	Foot Length (in)	Medial Malleoli Height (in)	Lateral Malleoli Height (in)
3	2.84	7.56	1.73	5.32	2.06	1.97
20-80	4.1478	15.6	2.91	10.59	3.55	3.02

The anthropometric data was used to determine the modular AFO components at both the upper and lower end of the size spectrum. The components at each bound were analyzed to ensure they met the failure criteria. The failure criteria analyzed for each AFO component were interface pressure, stiffness, and external moment.

In the sagittal plane, the AFO is required to resist moments generated by ankle inversion and eversion force couplings, foot adduction and abduction, and static foot alignment[32]. The literature did not provide quantitative information relating to the magnitude of the corrective forces required to at each specific location along the foot. Therefore, the interface pressure was considered sufficient to represent the magnitude of the corrective forces the AFO was required to apply at each respective location. The interface pressure was defined as the pressure from the contact of the AFO with the patient's soft tissue. The interface pressure was measured for each region of the inner planter mid-foot, inner medial metatarsal, and the ankle/side of heel regions, as shown in Figure 2.14[45]. Table 2.5 outlines the average pressures applied by each AFO section during gait.

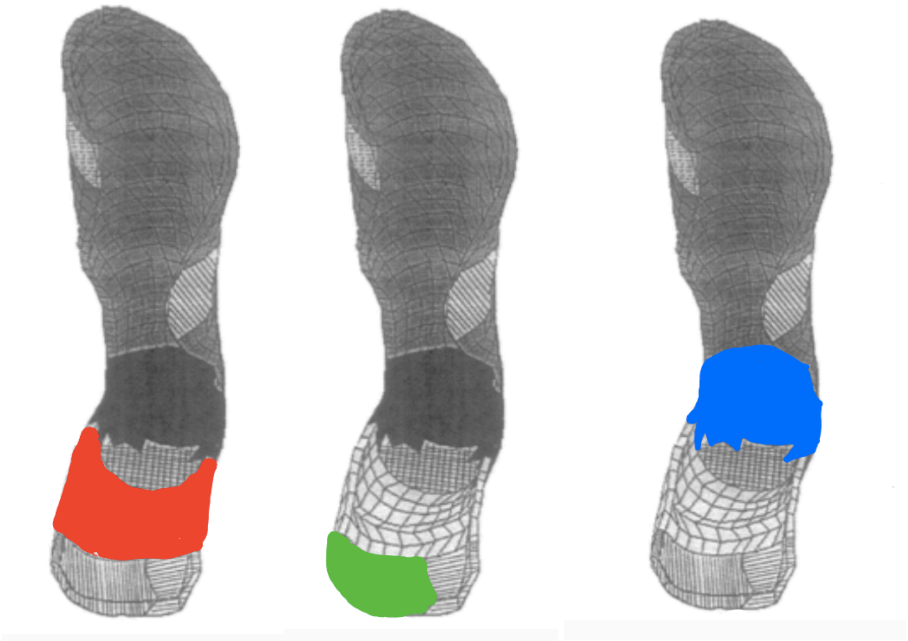

Figure 2.14: Location of interface pressure measurements:

A.Inner Plantar Mid-foot | B.Inner Medial Metatarsal | C.Ankle/Side of Heel[45]

Table 2.5: Average Pressures to Foot Regions During Gait[45]

Zone	Average Pressures (psi)
Inner Plantar Mid-Foot	5.76
Inner Medial Metatarsal	12.15
Ankle/Side of Heel	8.71

AFO torsional stiffness is important to providing the right magnitude of corrective moment to support the patient[50,51]. Table 2.6 outlines the average AFO stiffness required to provide proper support for each respective patient population.

Table 2.6: Overview of Ankle-Foot Orthosis Torsional Stiffness[50]

Age (years)	0-19	20-80	80+
AFO Stiffness $(\frac{in-lb}{deg})$	40.71 ± 12.4	50.44 ± 7.96	46.02 ± 6.46

To determine the torsional stiffness of the model, the support components of the AFO were analyzed using the Pennsylvania based company, ANSYS', finite element analysis software. The foot plate was fixed in all degrees of freedom and a point load of magnitude F was applied to the location of the calf band located distance R from the anatomical joint center (ACJ), as shown in Figure 2.15[52].

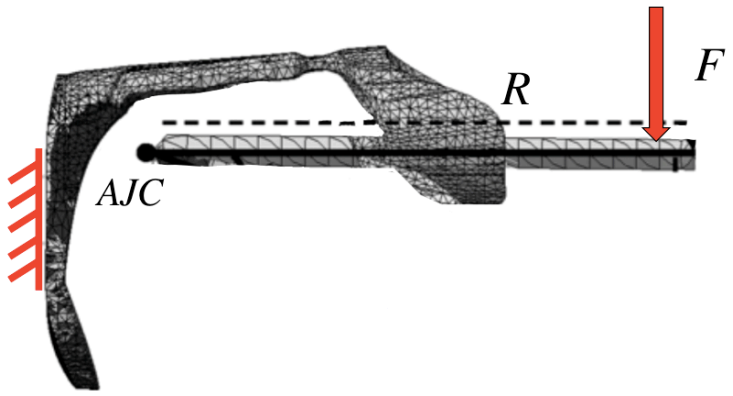

Figure 2.15: ANSYS Stiffness Model Boundary Conditions[52]

After completing the ANSYS model, the maximum vertical displacement (V_{dis}) of the AFO calculated by ANSYS (Figure 2.16), was used in Equation (2.3), to calculate the change in the shank-to-vertical angle (θ). The torsional stiffness of the AFO design was then calculated using Equation (2.4)[52].

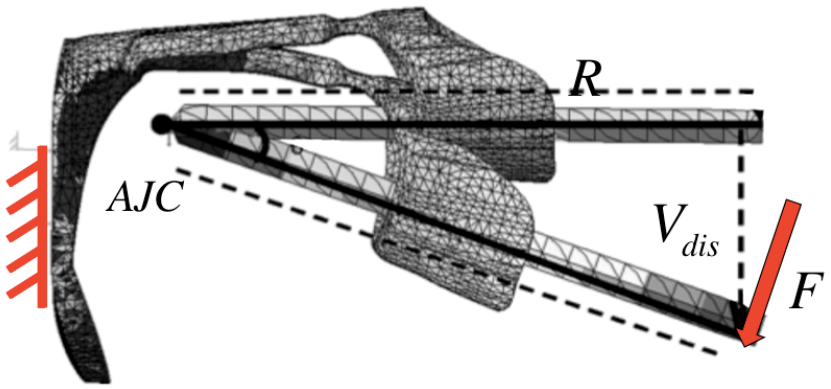

Figure 2.16: ANSYS Stiffness Model Vertical Displacement Output[52]

$$sin\theta = \frac{V_{dis}}{R} \tag{2.3}$$

$$Stiffness = \frac{F*R}{\theta} \tag{2.4}$$

The magnitude of the patient applied moment was also key for the design of failure resistance in the AFO, as it must be able to withstand moments equal to the maximum patient applied moment in both plantar flexion (Figure 2.17) and dorsiflexion (Figure 2.18)[44,53].

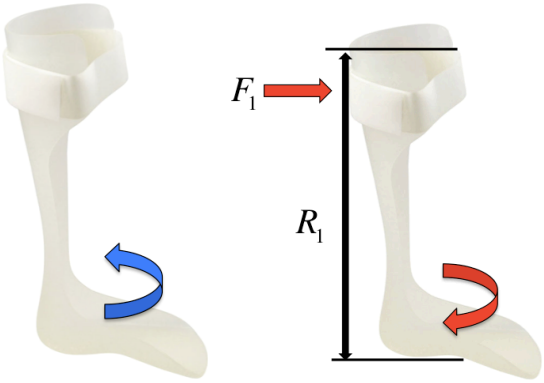

Figure 2.17: Plantar flexion (Blue) and Dorsiflexion Corrective Moment (Red)[53,54]

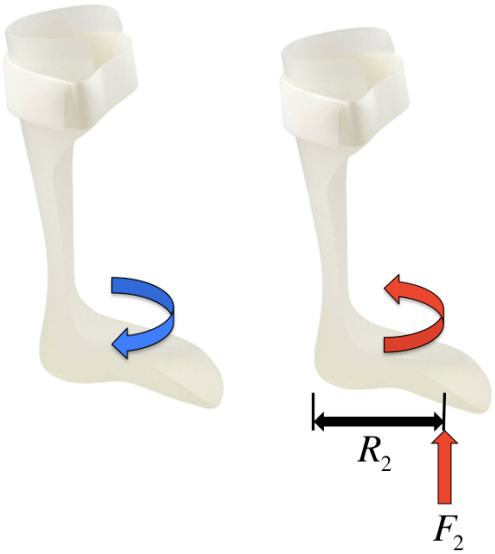

Figure 2.18: Dorsiflexion (Blue) and Plantar flexion Corrective Moment (Red)[53,54]

To evaluate the failure of the AFO, the magnitudes of the external ankle moments were estimated as 10 Nm for plantar flexion and 100 Nm for dorsiflexion for adult patients, and 50 Nm dorsiflexion for pediatric patients. The ankle moment magnitudes (E_m) were then applied to the distance to the top of proximal trimline (R) calculated from the anthropometric data to determine the reaction force at the calf-band interface (F) using Equation 2.5[53].

$$F = \frac{E_m}{R} \tag{2.5}$$

2.3 Evaluation of Functional Requirements

Based on the functional requirements, the modular AFO components were designed and assembled in SolidWorks (Figure 2.19). Each modular component was tested against failure criteria. Modular components with complex geometries were analyzed using the finite element analysis software ANSYS. The ANSYS software models used were structural with solid 10 node tetrahedral elements and isotropic materials. Model verification was completed using hand calculations and beam theory.

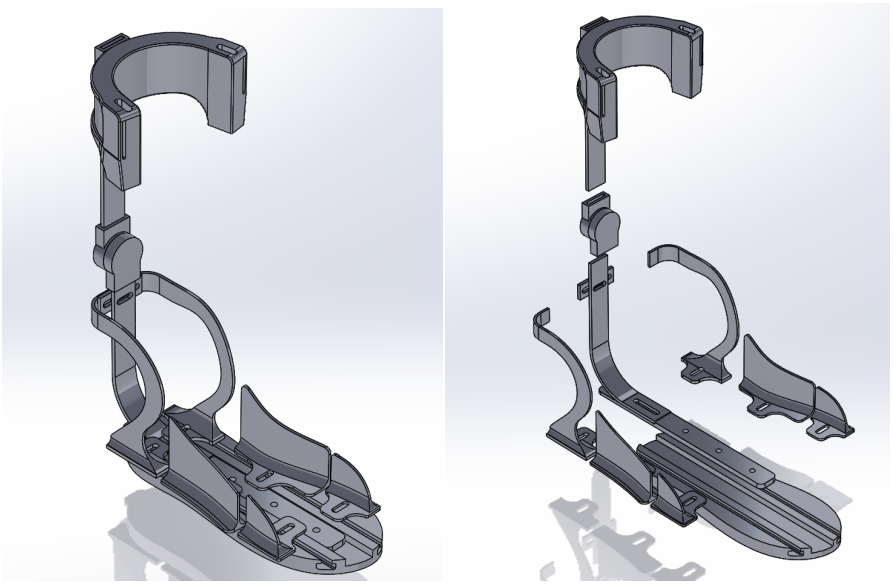

Figure 2.19: Assembly and Exploded View of Modular AFO components

2.3.1 Functional Requirements: Size

The anthropometric data was used to determine the size requirements of each component for a pediatric patient. The size of each modular component was determined by examining the required size range and determining the maximum and minimum parts that could fit each patient and meet the required support criteria.

The medial and lateral support components consisted of ankle, mid-foot, and metatarsal supports. The medial and lateral ankle supports were required to avoid the bony prominences of the medial and lateral malleoli, as well as, fall at least 1cm anterior to the malleoli[31–33]. Based on these sizing components, the height and width of the components (Figure 2.20) were determined and the results are summarized in Table 2.7.

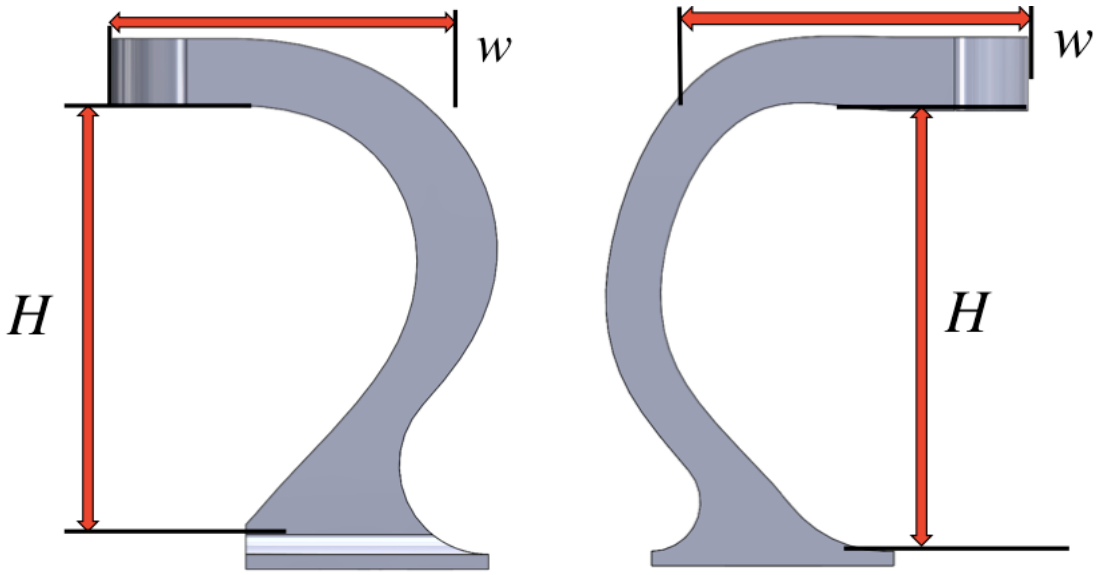

Figure 2.20: Lateral and Medial Ankle Support Components

Table 2.7: Pediatric Lateral and Medial Ankle Support Component Size Summary

		Lateral		Medial	
Model	Age Range	Height [H] (in)	Width [w] (in)	Height [H] (in)	Width [w] (in)
1	3	1.9	1.15	2	1.5
2	4-6	2.6	1.35	2.65	1.75
3	7-9	2.95	1.55	3	2
4	10-11	3.2	1.75	3.2	2.25

The lateral and medial mid-foot supports were required to be higher than the navicular height[31,32,38]. Based on these sizing components, the height of the components (Figure 2.21) were determined and the results are summarized in Table 2.8.

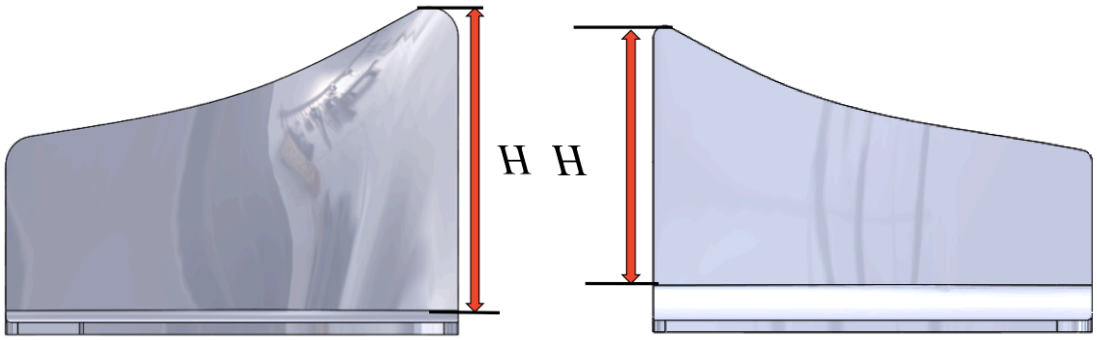

Figure 2.21: Lateral and Medial Mid-Foot Support Components

Table 2.8: Pediatric Lateral and Medial Mid-foot Support Component Size Summary

Model	Age Range	Height [H] (in)
1	3	1.75
2	4-6	2.0
3	7-10	2.5
4	11	2.75

The lateral and medial metatarsal supports were required to be higher than the 5th and 1st metatarsal height[31,32,38]. Based on these sizing components, the height of the components (Figure 2.22) were determined and the results are summarized in Table 2.9.

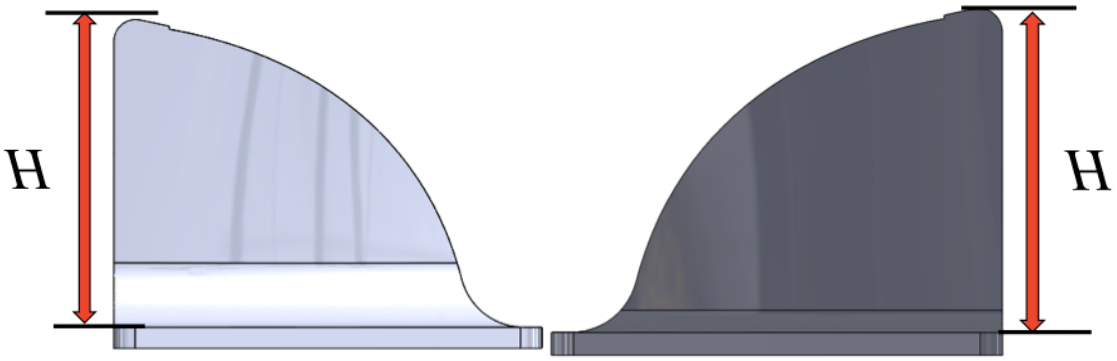

Figure 2.22: Lateral and Medial Metatarsal Support Components

Table 2.9: Pediatric Lateral and Medial Metatarsal Support Component Size Summary

		Lateral	Medial
Model	Age Range	Height [H] (in)	Height [H] (in)
1	3	1.0	1.0
2	4-6	1.2	1.15
3	7-10	1.5	1.5
4	11	1.75	1.6

The structural support components consisted of the foot bar, heel cup, and calf bar. The overall height of the calf bar and heel cup were required to remain 3.8 cm below the femoral head to avoid the peroneal nerve[32,40,41]. The heel cup height is required to sit at least 1 in higher than the patient navicualar[32,40]. Based on these sizing components, the height and of the components (Figure 2.23) were determined and the results are summarized in Table 2.10.

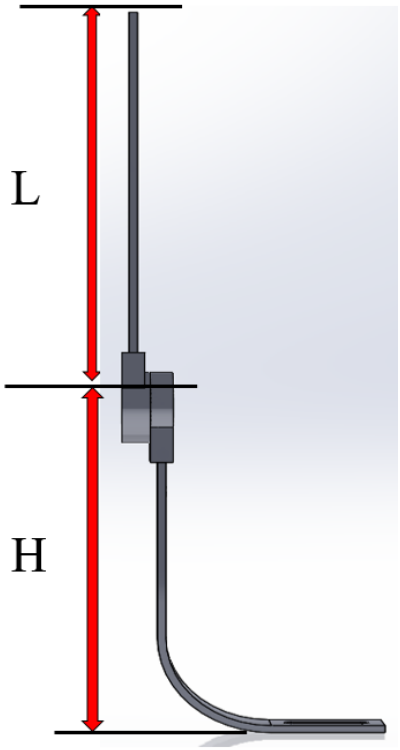

Figure 2.23: Dimensions of Heel Cup and Calf Bar

Table 2.10: Pediatric Heel Cup and Calf Bar Support Component Size Summary

Model	Age Range	Height [H] of Heel Cup (in)	Length [L] of Calf Bar (in)
1	3	2.75	4.75
2	4-5	3.0	5.5
3	6	3.0	5.75
4	7-8	3.5	6.25
5	9-10	3.5	7
6	11	3.75	7.5

The foot bar and footplate, shown in Figure 2.24, were sized based on the standard sizing chart for shoes which depend on the length of the foot[32]. To provide the proper support to counteract the plantar flexion moment the foot bar must extend to at least the head of the 1st metatarsal[55]. Based on these sizing components, the lengths of foot bar and footplate components were determined from standardized shoe lengths with the lower bound as the 3-year old male model (5.32 in) and the upper bound as the 11-year old female model (8.81 in). The shoe standard sizes that fell between the upper and lower bound were included. The results are summarized in Table 2.11.

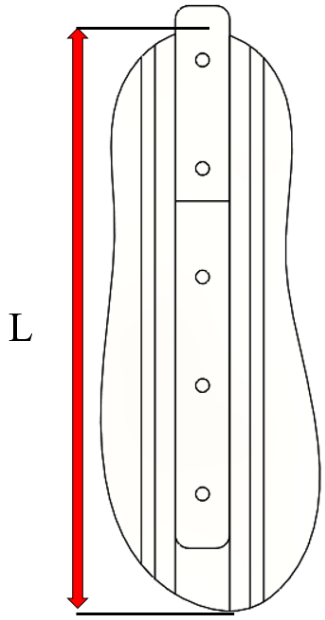

Figure 2.24: Foot Bar and Footplate Dimensions

Table 2.11: Pediatric Foot Bar and Footplate Component Size Summary

Model	Length [L] of Foot Bar (in)	Standard Shoe Size (US)
1	5.125	6C
2	5.5	7C
3	5.75	8C
4	6.125	9C
5	6.5	10C
6	6.75	11C
7	7.125	12C
8	7.5	13C
9	7.75	1Y
10	8.125	2Y
11	8.5	3Y
12	8.75	4Y
13	9.125	5Y

The calf band (Figure 2.25) was sized based on the patients' calf diameter[32]. Summaries of the calf band component sizes are shown below in Table 2.12.

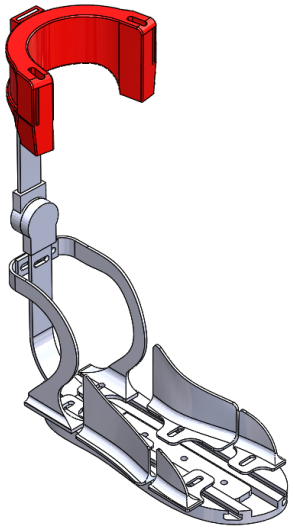

Figure 2.25: Modular AFO Calf Band

Table 2.12: Calf Band Size

Model	Age (Years)	Calf Band Diameter (in)
1	3	2.75
2	4-6	3.25
3	7-10	3.75
4	11	4

2.3.2 Functional Requirements: Failure Criteria

The modular components were created and scaled for the largest and smallest requirements of the patient range. ANSYS was used to complete failure analysis on the modular components with the loads outlined for each part consideration.

The critical component evaluation consisted of the medial/lateral mid-foot supports, the medial/lateral metatarsal supports, the medial/lateral ankle supports, and the overall AFO stiffness. Each support was modeled using 10 node tetrahedral elements with a mesh size of 0.125 in for the adult patients and 0.0625 in for the pediatric patients.

The mechanical properties used for each component were isotropic and varied based on the part. The calf bar, heel cup, and foot bar were modeled out of aluminum (Figure 2.26.A). The footplate was modeled out of Delrin, also known as polyoxymthylene (POM). The calf band was modeled out of polylactic acid (PLA). The medial and lateral support components (Figure 2.26.B) were modeled out of 30% acetal co-polymer glass fiber.

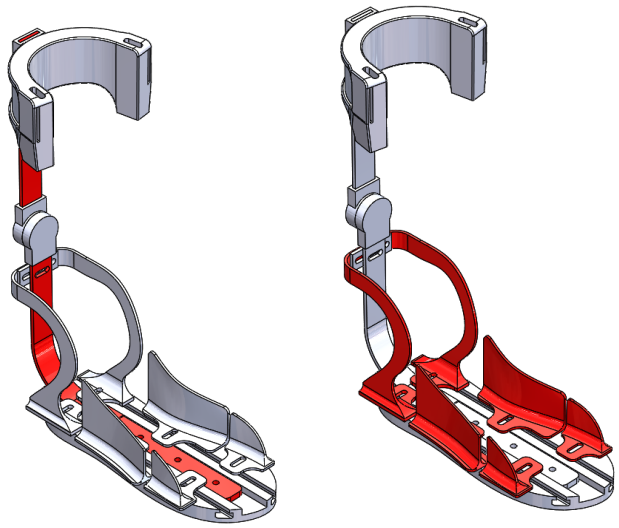

Figure 2.26: A. AFO structural support components

B. AFO Medial/Lateral support components

Each of the materials chosen for the modular components was considered based on potential manufacturing methods and mechanical properties. A summary of the ANSYS input values for the elastic modulus and Poisson's ratio is shown in Table 2.13.

Table 2.13: Summary of ANSYS material model input values

Material	Elastic Modulus (psi)	Poisson's Ratio	Yield Strength (psi)
Delrin	675000	0.35	8700
30% Acetal Co-polymer Glass Fiber	1200000	0.35	16000
Aluminum	10000000	0.33	40000

Each critical modular component was evaluated against the failure criteria. The footplate component was modeled in SolidWorks out of Delrin. The stress in the footplate was calculated using the weight of the patient (W) and the area of the footplate (A) equation 2.5 . Table 2.14 summarizes the resulting normal stress for each model.

$$\sigma = \frac{W}{A} \tag{2.5}$$

Table 2.14: Parameters for 3-year old and Adult patients

Model	Normal Stress (psi)
3-year old male	8.32
Adult male	18.67

The medial and lateral ankle support plates were modeled out of acetal copolymer with 30% glass fiber reinforcement. The bottom of the plate was constrained in all degrees of freedom to simulate the interface with the footplate. Constraints were also applied to account for the support strap, as shown by the red regions in Figure 2.27. The medial and lateral ankle support experience an interface pressure at the ankle/side of heel region of 8.17 psi, as shown by the blue region in Figure 2.27[45].

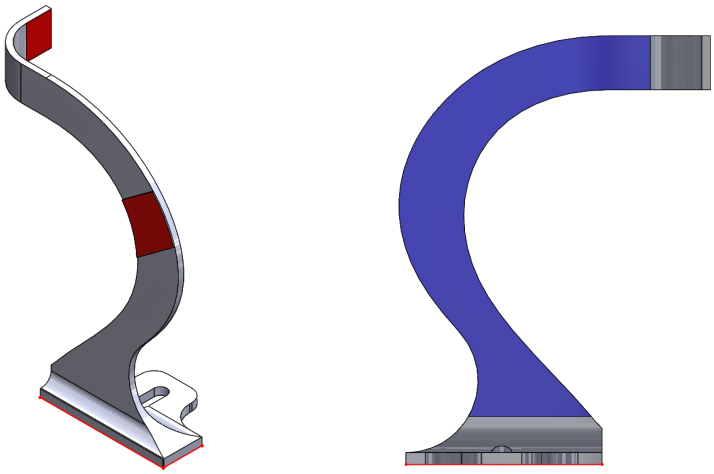

Figure 2.27: Constraints (Red) and Loads (Blue) applied to Ankle Support Plates

The ANSYS analysis revealed a maximum von mises stress of 5899.33 psi and a maximum displacement of 0.006154 in for the pediatric lateral ankle support plate (Figure 2.28).

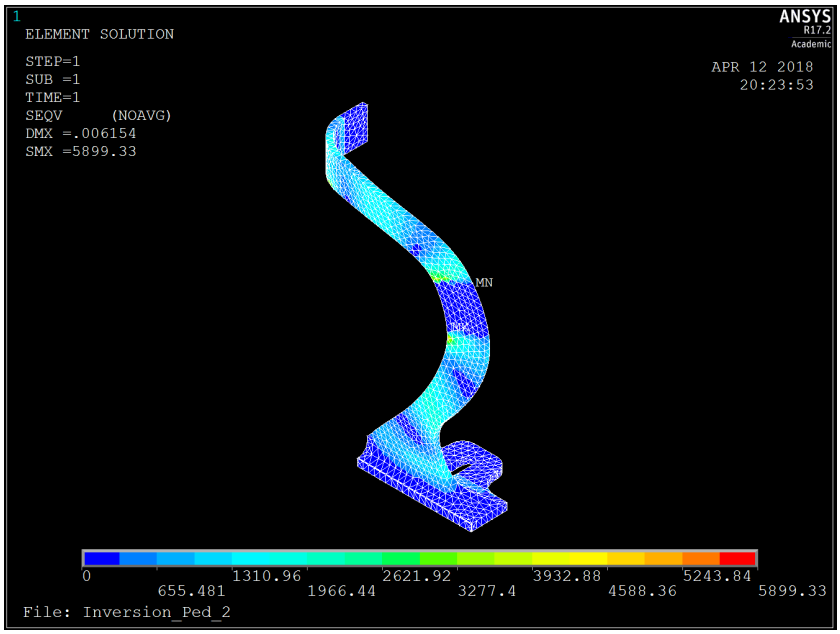

Figure 2.28: Lateral Ankle Support Plate Von Mises Stress Contour Plot

The ANSYS analysis revealed a maximum von mises stress of 9491.79 psi and a maximum displacement of 0.008681 in for the pediatric medial ankle support plate (Figure 2.29).

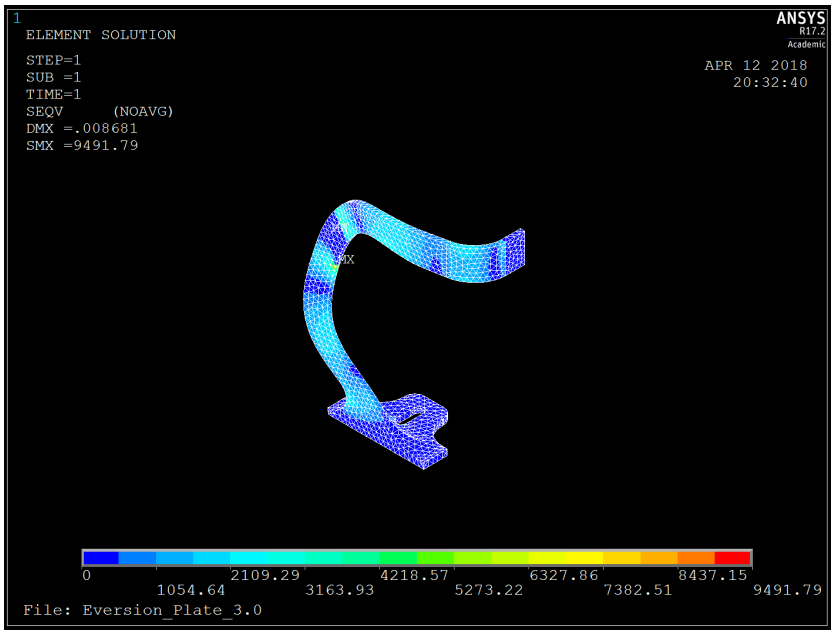

Figure 2.29: Medial Ankle Support Plate Von Mises Stress Contour Plot

The medial and lateral mid-foot support plates were modeled using acetal copolymer with 30% glass fiber reinforcement. The medial mid-foot support plate experiences the interface pressure at the plantar mid-foot region region of 5.76 psi. The model was constrained in all degrees of freedom along the bottom area and the interface pressure was applied to each respective face Figure 2.30[45].

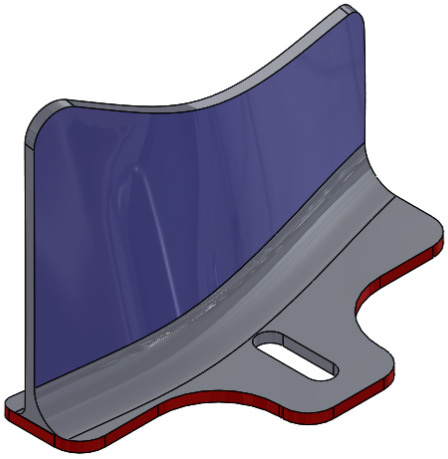

Figure 2.30: Constraints (Red) and Loads (Blue) applied to Mid-foot Support Plates

The ANSYS analysis revealed a maximum von mises stress of 5735.63 psi and a maximum displacement of 0.029621 in for the pediatric medial mid-foot support plate (Figure 2.31).

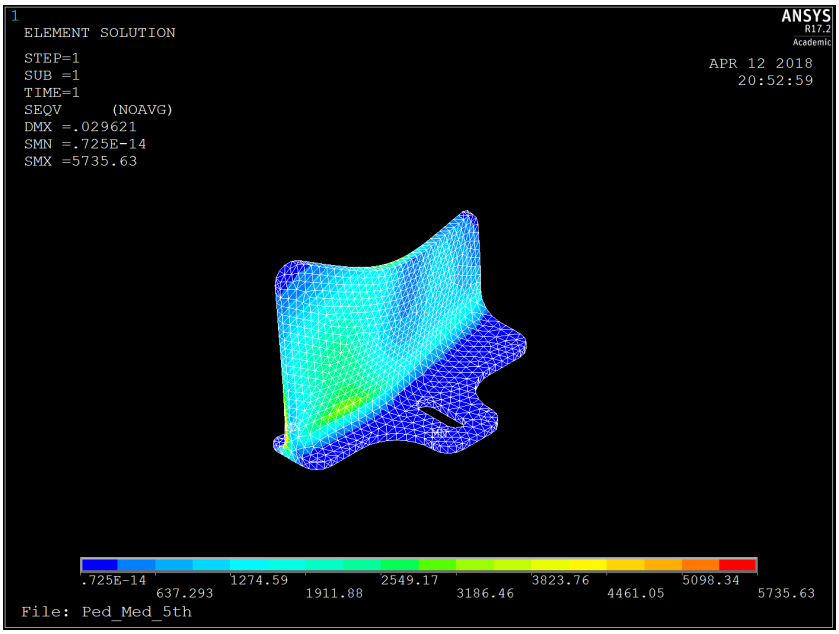

Figure 2.31: Lateral Mid-Foot Support Plate Von Mises Stress Contour Plot

The ANSYS analysis revealed a maximum von mises stress of 5296.18 psi and a maximum displacement of 0.030268 in for the pediatric lateral mid-foot support plate (Figure 2.32).

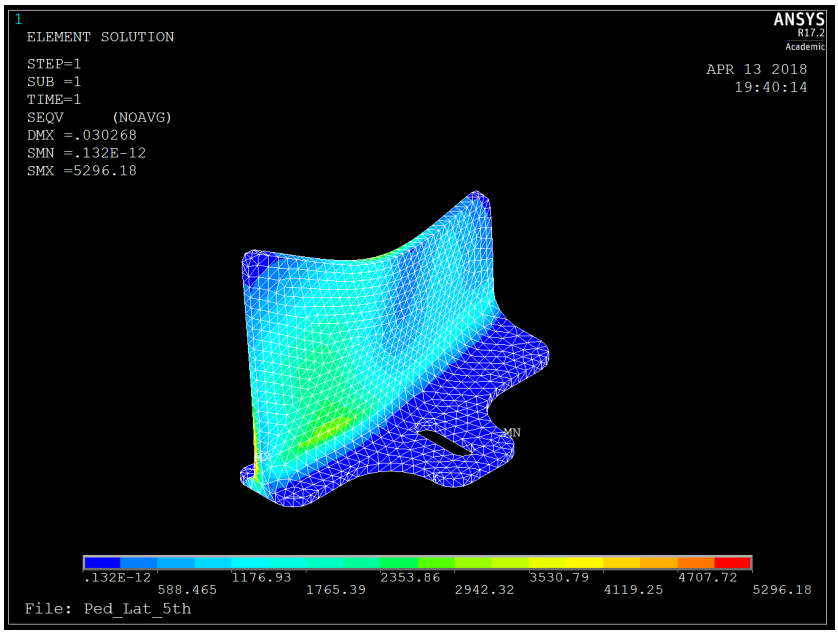

Figure 2.32: Medial Mid-Foot Support Plate Von Mises Stress Contour Plot

The medial and lateral metatarsal support plates were modeled as acetal copolymer with 30% glass fiber reinforcement. A displacement boundary condition constraining all degrees of freedom was applied to the lower face of the plate (Figure 2.33). The medial and lateral metatarsal support plate experienced an interface pressure at the inner metatarsal region of 12.15 psi[45].

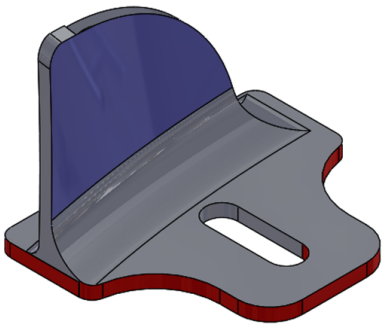

Figure 2.33: Constraints (Red) and Loads (Blue) applied to Metatarsal Support Plates

The ANSYS analysis revealed a maximum von mises stress of 5735.63 psi and a maximum displacement of 0.029621 in for the pediatric medial metatarsal support plate (Figure 2.34).

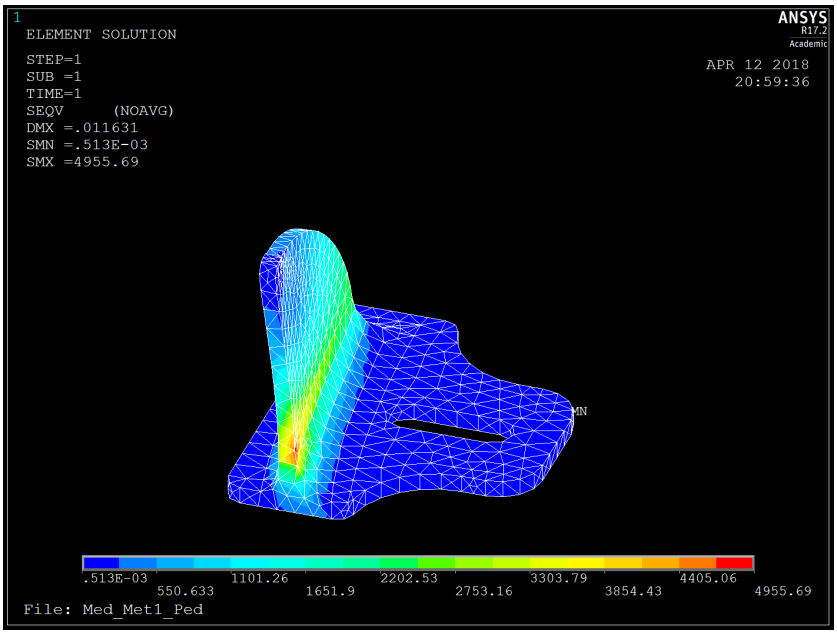

Figure 2.34: Medial Metatarsal Support Plate Von Mises Stress Contour Plot

The ANSYS analysis of the pediatric lateral metatarsal support plate revealed a maximum von mises stress of 4619.54 psi and a maximum displacement of 0.010101 in (Figure 2.35).

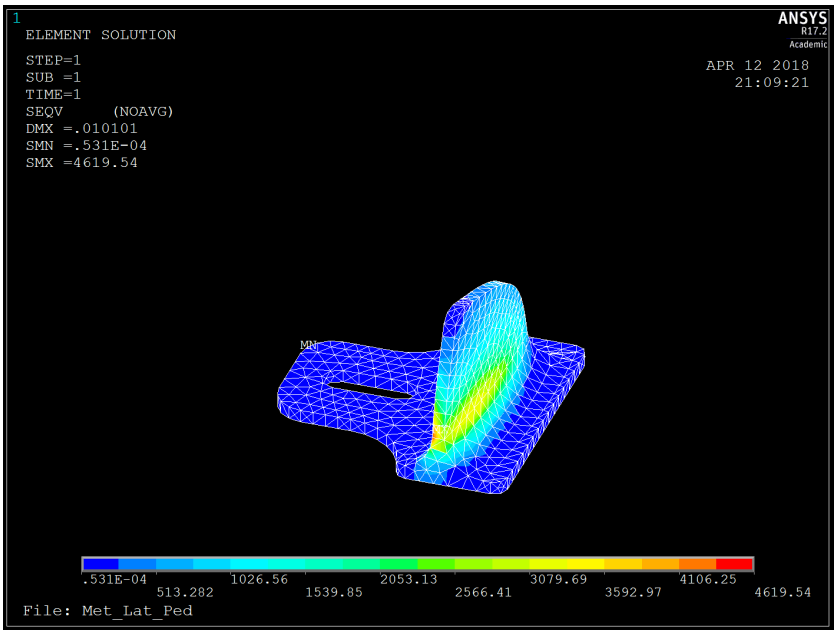

Figure 2.35: Lateral Metatarsal Support Plate Von Mises Stress Contour Plot

ANSYS simulations were also completed for the adult male model AFO using a 0.125 in mesh. The results are for maximum von mises stress and deflection are listed below in Table 2.15.

Table 2.15: ANSYS Outputs for Adult AFO Component Analysis

Part	Max Von Mises Stress (psi)	Max Deflection (in)
Medial Metatarsal	4959.8	0.0000520
Lateral Metatarsal	4618.98	0.0000531
Medial Mid-Foot	5736.12	0.000695
Lateral Mid-Foot	5834.12	0.000743
Medial Ankle	8214.54	0.016097
Lateral Ankle	9068.62	0.018943

The torsional stiffness and external moment were determined by modeling the support components consisting of the calf bar, heel cup, and foot bar in ANSYS as aluminum. The foot bar of the AFO was fixed in all degrees of freedom, while a point load, equal to the magnitude required to counteract the external moment, was applied at the top of the proximal calf (Figure 2.36)[52].

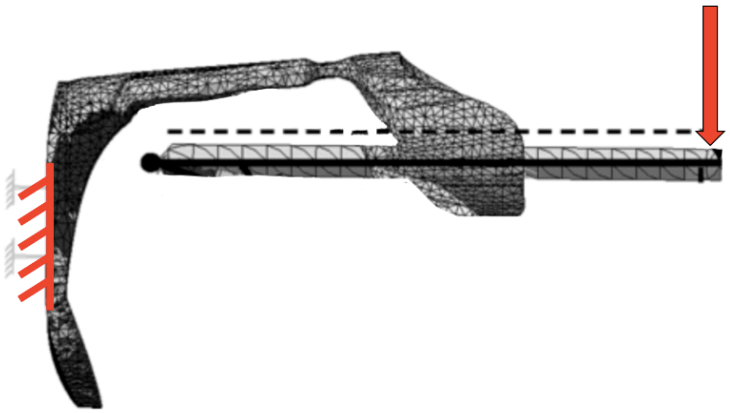

Figure 2.36: Boundary and Loading Conditions for AFO assembly[52]

The ANSYS analysis revealed a maximum displacement of 1.05721 in (Figure 2.37) and a maximum von mises stress of 15408.5 psi (Figure 2.38). The displacement resulted in a calculated AFO stiffness of 47.32 ($\frac{in-lb}{deg}$). Table 2.16 summarizes the results for the AFO torsional stiffness.

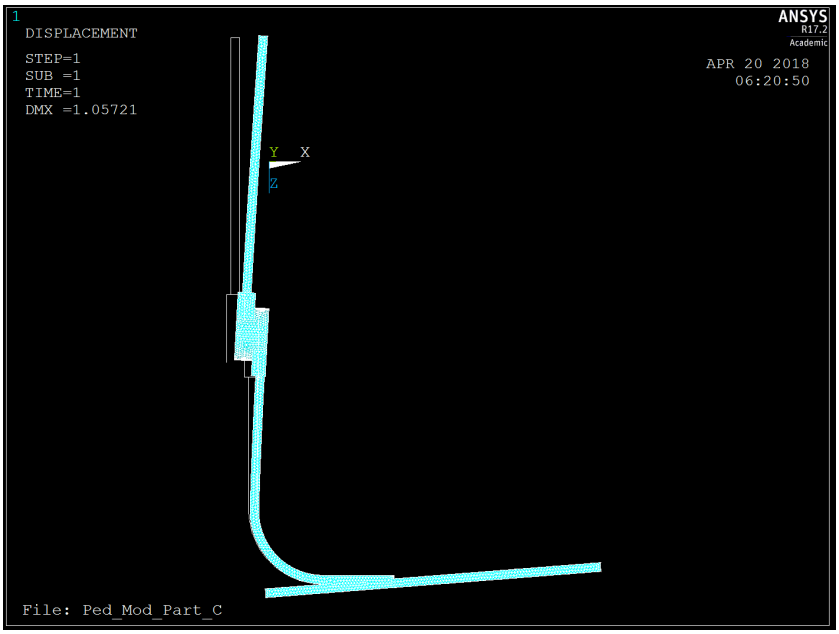

Figure 2.37: Deflection Plot of AFO Stiffness

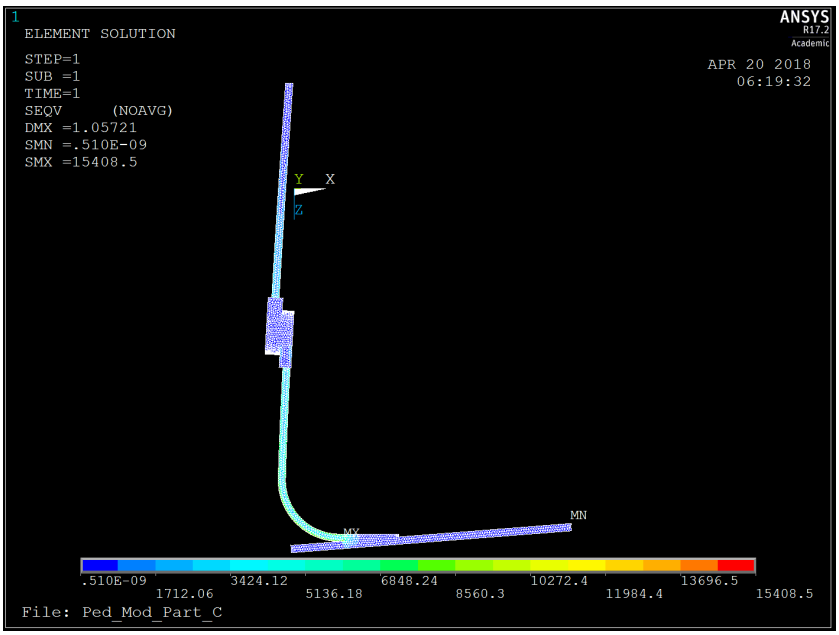

Figure 2.38: Von Mises Stress Contour Plot of Externally Applied Moment

Table 2.16: Modular AFO Calculated Torsional Stiffness Results

Model	3-year old male	Adult male
AFO Stiffness $(\frac{in-lb}{deg})$	47.32	54.93

2.4 FEA Validation

To validate the model stress and deflection analysis outputs from ANSYS software, hand calculations were completed. The boundary conditions used in the ANSYS model are similar to that of a cantilevered beam with a rectangular cross-section. The maximum bending stress (σ) was calculated from Equation 2.6 using the vertical distance from the neutral axis (y), the moment of inertia for a rectangular cross-section (I), and the calculated bending moment (M). The maximum deflection (δ_{max}) was

calculated from Equation 2.7 using the distributed load per unit length (w), the material Young's Modulus (E) and the moment of intertie about the neutral axis (I).

$$\sigma = \frac{My}{I} \tag{2.6}$$

$$\delta_{max} = \frac{wl^4}{8EI} \tag{2.7}$$

The results from the hand calculations are shown below in Table 2.17. Because the parts were scaled to create the pediatric and adult models, the maximum stress and deflection remained the same for both models.

Table 2.17: Summary of Hand Calculation Results

Part	w (lb/in)	σ (psi)	δ_{max}(in)
Medial Metatarsal	0.6075	6339.13	0.0000522
Lateral Metatarsal	0.0674	5607.7	0.0000754
Medial Mid-Foot	0.2304	2707.2	0.000686
Lateral Mid-Foot	0.2592	2526.3	0.000465
Medial Ankle	0.6075	5594.05	0.0000113
Lateral Ankle	0.0674	7843.20	0.0000568

The results of the maximum von mises stress and maximum deflection from the ANSYS simulation had some differences from the hand calculations. In the metatarsal region, the hand calculations predicted a stress about 1.25 times greater than the ANSYS model output. This difference was likely due to the cross-section taken for the moment of

inertia. The smallest cross section of the metatarsal parts was taken to determine the maximum stress of the part. Therefore, because the ANSYS reported stress is less than the hand-calculated value, the stress output is likely valid. In the mid-foot region, the ANSYS reported von mises stress was much larger than the stress reported from the hand calculations. This difference is likely due to the complex curvature of the mid-foot parts required to align to the foot geometry. The cantilever beam equations do not take the curvature into account and, therefore, would report a lower maximum stress. In the heel region, the ANSYS analysis reported a value about 1.25 times larger than the hand calculated values. Once again, this difference is likely due to the complex geometry and stress concentration due to the geometry of the part. In all regions, the maximum deflection closely matched the value from the hand calculations. All modular components passed the failure analysis.

Chapter 3: Discussion

The purpose of this study was to design a highly customizable and low-cost modular AFO with easily interchangeable components. This study was, to the best of our knowledge, the first attempt at creating a modular ankle-foot orthosis. The modular components were designed based on the support requirements of modular design, easily interchangeable components, and low-cost (less than $200).

3.1 Modular Components

The final AFO design consisted of 62 modular components. Each designed to support a different portion of the foot-ankle complex to allow for the required correction of gait impairment. The footplate cross-section was designed similar to that of structural aluminum to allow movement in the x and y directions for the placement of the medial and lateral support plates. The foot strut connects to the footplate using screws, this allows the foot bar freedom in the y-direction to be positioned in the desired position along the footplate. The design of the posterior support components contained a calf bar and a heel cup. The heel cup connected to the foot strut using screws. A connector was modelled between the calf bar and heel cup, to allow for the material and sizing of both the heel cup and calf bar to be changed independently. The combination of the foot bar, heel cup, and calf bar allow for tuning of the overall stiffness of the AFO.

3.2 Easily Interchangeable Components

The final AFO design was to consist of easily interchangeable components. However, due to the absence of a physical prototype, this objective was difficult to test. The modular components were designed with the intent to be easily placed and maneuvered. Figure 3.1 shows the combinations of modular components that can be combined to treat ankle inversion and eversion, demonstrating the potential of the components to be interchangeable.

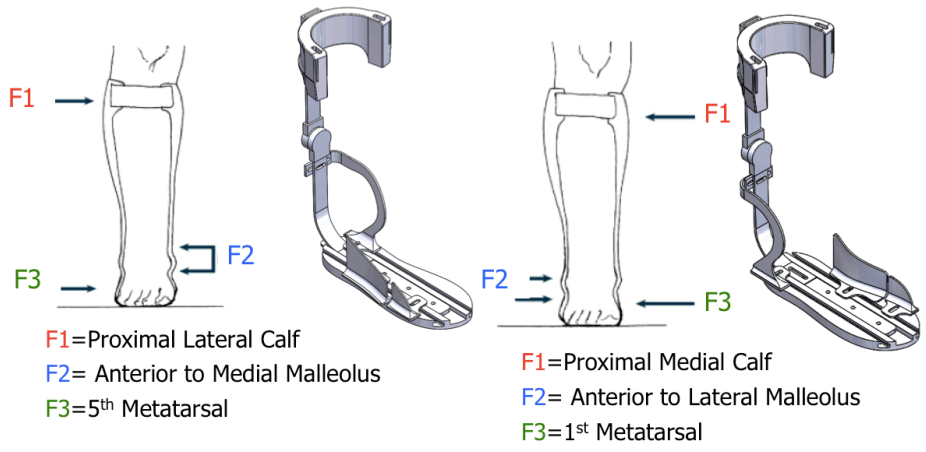

Figure 3.1: Modular Components to Treat Ankle Inversion/Eversion[32]

3.3 Low-Cost: Materials

Another important aspect of the modular AFO component design was the selection of the materials. The selected material for each part was required to meet the mechanical requirements for the applied load, as well as, biocompatible, lightweight, and inexpensive. Biocompatible components are FDA approved for prolonged human use. To

keep the cost of the AFO down, the components were required to be easy to manufacture. The materials were also selected for compatibility with injection molding and 3-D Printing. Table 3.1 lists the price of the selected materials and potential manufacturing methods for each.

Table 3.1: Summary of Material Cost and Manufacturing Methods[56]

Material	Price (per cubic inch)	Manufacturing Method
Aluminum	$0.87	Machining Extrusion
Delrin (POM)	$3.28	3-D Printing Injection Molding
PLA	$0.83	3-D Printing Injection Molding
Acetal 30% Glass Fiber	$2.36	3-D Printing Injection Molding

3.4 Limitations

In this study there were several limitations that should be considered. First, the corrective forces applied by the AFO were not well-documented, so average interface pressures from a healthy adult population were used. In cases where the patient has excessive deformity, it is possible that these interface pressures would not be representative. The interface pressures may also differ among the adult and pediatric population, however, any potential discrepancies have, to the best of our knowledge, yet to be explored. Second, this study examined populations ranging for 3-11 and over 20 years due to the lack of anthropometric data for the 12-19 year age group. However, the 12-19 year group is still contained in the upper and lower bounds provided by the 3-year old male and adult male models.

4. Conclusions

4.1 Contributions

Traditional custom AFOs are expensive and time consuming to produce, while prefabricated AFOs are unable to meet the support requirements for a majority of patients[1,8]. A modular AFO would allow for a higher level of customization with the potential for a substantially less production time and cost. The process of designing a modular AFO required quantitative metrics to determine the functional requirements. While the literature outlines the qualitative process of AFO design, there was a distinct lack of compiled quantitative information. The results of this study provide a compilation of the size and support requirements for both pediatric and adult AFO design, as well as, a completed model of a modular AFO.

4.2 Future Work

In order to better understand how the modular AFO design interacts with the patient and the pedorthist, a prototype should be created. The prototype of the modular AFO design should be evaluated for manufacturing cost, ease of assembly, and repeatability. The ease of assembly would be evaluated through a time study of the assembly process and pedorthist feedback. Test subject and pedorthist feedback would be used to compare patient fit. Load cells would be used to evaluate the AFO for the effectiveness of force application at the initial fitting.

One of the limitations of this study was the lack of information regarding force application requirements of AFOs for a more diverse population. More studies

investigating how AFOs provide support to different patient population specifically quantitate force and geometry information, should be conducted.

4.3 Summary

SolidWorks was used to create a modular AFO that met the determined functional requirements of size and failure criteria for a large portion of the patient population. ANSYS finite element analysis software was used to analyze the individual components to ensure they could meet the functional requirements. The modular AFO design consisted of 14 components. The critical components were further divided based on size requirements to generate a set of 62 interchangeable parts that could be used to build an AFO for pediatric patients ages 3-11 years. This research serves as an important first step to developing modular assistive devices and lowering the financial burden placed on patients.

References:

1. Whiteside, S. *et al.* Practice Analysis of Certified Practitioners in the Disciplines of Orthotics and Prosthetics. *Certif. Orthotics, Prosthetics Pedorth.* 42 (2007).
2. LeBlanc, M. A. Patient population and other estimates of prosthetics and orthotics in the USA. *Orthot. Prosthetics* **27,** 38–44 (1973).
3. Munguia, J. & Dalgarno, K. Ankle-foot orthotics optimization by mens of composite reinforcement of free-form structures. *24th Int. SFF Symp. Addit. Manuf. Conf.* **SFF,** 766–776 (2013).
4. Kitaoka, H. B. *et al.* The effect of custom-made braces for the ankle and hindfoot on ankle and foot kinematics and ground reaction forces. *Arch. Phys. Med. Rehabil.* **87,** 130–135 (2006).
5. Shorter, K. A., Xia, J., Hsiao-Wecksler, E. T., Durfee, W. K. & Kogler, G. F. Technologies for Powered Ankle-Foot Orthotic Systems: Possibilities and Challenges. *IEEE/ASME Trans. Mechatronics* **18,** 337–347 (2013).
6. Nieveen, N. & Akker, J. Van Den. Exploring the Potential of. **3,** 27–37 (1999).
7. Neville, C. & Houck, J. Choosing Among 3 Ankle-Foot Orthoses for a Patient With Stage II Posterior Tibial Tendon Dysfunction. *J. Orthop. Sport. Phys. Ther.* **39,** 816–824 (2009).
8. Mavroidis, C. *et al.* Patient specific ankle-foot orthoses using rapid prototyping. *J. Neuroeng. Rehabil.* **8,** 1 (2011).
9. AFO Force Application. Available at: https://fadavispt.mhmedical.com/data/books/1865/ch_fig-2-10.png.
10. Malas, B. S. What variables influence the ability of an AFO to improve function and when are they indicated? *Clin. Orthop. Relat. Res.* **469,** 1308–1314 (2011).
11. Wingstrand, M., Hägglund, G. & Rodby-Bousquet, E. Ankle-foot orthoses in children with cerebral palsy: a cross sectional population based study of 2200 children. *BMC Musculoskelet. Disord.* **15,** 327 (2014).
12. AFO Casting. Available at: .
13. Lautenschlager E, Bayne S, Wildes R, Russ J, Yanke M. Materials investigation of failed plastic ankle-foot orthoses. *J. Orthot. Prosthetics* **29,** 25–27 (1975).
14. Bregman, D. J. J. *et al.* A new method for evaluating ankle foot orthosis characteristics: BRUCE. *Gait Posture* **30,** 144–149 (2009).
15. Pawale, A. A. Review: Analysis and Manufacturing of Ankle Foot Orthosis for Foot Drop. *IOSR J. Mech. Civ. Eng.* **17,** 12–15 (2017).
16. Jin, Y., He, Y. & Shih, A. Process Planning for the Fuse Deposition Modeling of Ankle-Foot-Othoses. *Procedia CIRP* **42,** 760–765 (2016).
17. Chen, R. K., Jin, Y. an, Wensman, J. & Shih, A. Additive manufacturing of custom orthoses and prostheses-A review. *Addit. Manuf.* **12,** 77–89 (2016).
18. Walbran, M., Turner, K. & McDaid, A. J. Customized 3D printed ankle-foot

orthosis with adaptable carbon fibre composite spring joint. *Cogent Eng.* **3,** 1–11 (2016).
19. Totah, D., Kovalenko, I., Saez, M. & Barton, K. Manufacturing Choices for Ankle-Foot Orthoses: A Multi-objective Optimization. *Procedia CIRP* **65,** 145–150 (2017).
20. Aboutorabi, A., Arazpour, M., Ahmadi Bani, M., Saeedi, H. & Head, J. S. Efficacy of ankle foot orthoses types on walking in children with cerebral palsy: A systematic review. *Ann. Phys. Rehabil. Med.* **60,** 393–402 (2017).
21. Devices, A. Fact Sheet: Foundations of Pediatric Orthotics. 1–7 (2009).
22. Fryar, C. D., Gu, Q. & Ogden, C. L. *Anthropometric reference data for children and adults: United States, 2007-2010. Vital and health statistics. Series 11, Data from the national health survey* (2012). doi:10.1186/1471-2431-8-10
23. Westberry, D. E. *et al.* Impact of ankle-foot orthoses on static foot alignment in children with cerebral palsy. *J. Bone Jt. Surg. - Ser. A* **89,** 806–813 (2007).
24. Morris, C. & Orth, S. R. Orthotic Management of Children with Cerebral Palsy. *Jpo* **14,** 1–9 (2002).
25. Abel, M. F., Juhl, G. A., Vaughan, C. L. & Damiano, D. L. Gait assessment of fixed ankle-foot orthoses in children with spastic diplegia. *Arch. Phys. Med. Rehabil.* **79,** 126–133 (1998).
26. Equinus Deformity.
27. Crouch Gait.
28. Butler, P. B. & Nene, A. V. The Biomechanics of Fixed Ankle Foot Orthoses and their Potential in the Management of Cerebral Palsied Children. *Physiotherapy* **77,** 81–88 (1991).
29. Critical Joints.
30. Ries, A. J., Novacheck, T. F. & Schwartz, M. H. A data driven model for optimal orthosis selection in children with cerebral palsy. *Gait Posture* **40,** 539–544 (2014).
31. Pratt, D. J. & Sanner, W. H. Paediatric foot orthoses. *Foot* **6,** 99–111 (1996).
32. Lusardi, M. M., Jorge, M. & Nielsen, C. C. *Orthotics & prosthetics in rehabilitation*. (Elsevier Saunders, 2013).
33. Takahashi, S. & Shrestha, A. The Vulpius procedure for correction of equinus deformity in patients with hemiplegia. *J. Bone Joint Surg. Br.* **84–B,** 978–980 (2002).
34. Foot and Ankle. Available at: https://encrypted-tbn0.gstatic.com/images?q=tbn:ANd9GcS4MwkqSRUw079I6G_dAC7zIDiyURnlKHw-DFrpPp_83QyDJ6pB.
35. Yalla, S. V. *et al.* An immediate effect of custom-made ankle foot orthoses on postural stability in older adults. *Clin. Biomech.* **29,** 1081–1088 (2014).
36. Adduction. Available at: https://daniz53y71u1s.cloudfront.net/products/ADduction.png.
37. Abduction.
38. Lee, Y. S. *et al.* Plastic Ankle Foot Orthosis for Hemiplegics and Structural Analysis. *Key Eng. Mater.* **326–328,** 855–858 (2006).
39. Marx, H. W. LOWER-LIMB ORTHOTIC DESIGNS FOR THE SPASTIC HEMIPLEGIC PATIENT.

40. Lenhart, R. L. & Lenhart, R. Design of Improved Ankle-Foot Orthosis Senior Design Project. (2008).
41. Rodda, J. & Graham, H. K. Classification of gait patterns in spastic hemiplegia and spastic diplegia: a basis for a management algorithm. *Eur. J. Neurol.* **8,** 98–108 (2001).
42. IA, S. A sore spot in pediatrics: risk factors for pressure ulcers. *Pediatric Nursing* **29,** 278–282 (2003).
43. Sumiya, T., Suzuki, Y. & Kasahara, T. Stiffness control in posterior-type plastic ankle-foot orthoses: effect of ankle trimline. Part 1: A device for measuring ankle moment. *Prosthet. Orthot. Int.* **20,** 129–31 (1996).
44. Condie, D. N. & Meadows, C. B. Some Biomechanical Considerations In The Design Of Ankle-Foot Orthoses. *Orthot. Prosthetics* **31,** 45–52 (1977).
45. Nowak, M. D., Abu-Hasaballah, K. S. & Cooper, P. S. Design enhancement of a solid ankle-foot orthosis: real-time contact pressures evaluation. *J. Rehabil. Res. Dev.* **37,** 273–81 (2000).
46. Park, B.-K. & Reed, M. P. Parametric body shape model of standing children aged 3–11 years. *Ergonomics* **58,** 1714–1725 (2015).
47. Reed, M. P., Raschke, U., Tirumali, R. & Parkinson, M. B. Developing and Implementing Parametric Human Body Shape Models in Ergonomics Software. *3rd Digit. Hum. Model. Symp.* 1–8 (2014).
48. Park, B.-K., Lumeng, J. C., Lumeng, C. N., Ebert, S. M. & Reed, M. P. Child body shape measurement using depth cameras and a statistical body shape model. *Ergonomics* **58,** 301–309 (2015).
49. Fredriks, A. M. Nationwide age references for sitting height, leg length, and sitting height/height ratio, and their diagnostic value for disproportionate growth disorders. *Arch. Dis. Child.* **90,** 807–812 (2005).
50. Rosenberg, M. & Steele, K. M. Simulated impacts of ankle foot orthoses on muscle demand and recruitment in typically-developing children and children with cerebral palsy and crouch gait. *PLoS One* **12,** e0180219 (2017).
51. Kobayashi, T., Leung, A. K. L., Akazawa, Y. & Hutchins, S. W. Design of a stiffness-adjustable ankle-foot orthosis and its effect on ankle joint kinematics in patients with stroke. *Gait Posture* **33,** 721–723 (2011).
52. Schrank, E. S., Hitch, L., Wallace, K., Moore, R. & Stanhope, S. J. Assessment of a Virtual Functional Prototyping Process for the Rapid Manufacture of Passive-Dynamic Ankle-Foot Orthoses. *J. Biomech. Eng.* **135,** 101011 (2013).
53. McHugh, B. Analysis of body-device interface forces in the sagittal plane for patients wearing ankle-foot orthoses. *Prosthet. Orthot. Int.* **23,** 75–81 (1999).
54. Plastic AFO.
55. Stills, M. THERMOFORMED ANKLE-FOOT ORTHOSES.
56. Material Prices.